

UNCLASSIFIED

AD 262 888

*Reproduced
by the*

ARMED SERVICES TECHNICAL INFORMATION AGENCY
ARLINGTON HALL STATION
ARLINGTON 12, VIRGINIA



UNCLASSIFIED

NOTICE: When government or other drawings, specifications or other data are used for any purpose other than in connection with a definitely related government procurement operation, the U. S. Government thereby incurs no responsibility, nor any obligation whatsoever, and the fact that the Government may have formulated, furnished, or in any way supplied the said drawings, specifications, or other data is not to be regarded by implication or otherwise as in any manner licensing the holder or any other person or corporation, or conveying any rights or permission to manufacture, use or sell any patented invention that may in any way be related thereto.

88622

CATALOGED BY ASTIA

By

R. C. German and R. C. Bauer
RTF, ARO, Inc.

August 1961

ARNOLD ENGINEERING DEVELOPMENT CENTER

AIR FORCE SYSTEMS COMMAND



ASTIA
INSTRUMENT VENT
JUNE 1967

EFFECTS OF DIFFUSER LENGTH
ON THE PERFORMANCE OF EJECTORS
WITHOUT INDUCED FLOW

By

R. C. German and R. C. Bauer
RTF, ARO, Inc.

August 1961

AFSC Program Area 750G, Project 6950, Task No. 69501
ARO Project No. 100928

Contract No. AF 40(600)-800 S/A 24(61-73)

ABSTRACT

An investigation of ejectors without induced flow was made to determine the effects of varying diffuser lengths on ejector performance. Four 18-deg half angle conical nozzles having constant exit diameters and different throat diameters and two contoured nozzles having zero-deg half angles at the exit were used as the ejector driving nozzles. Unheated air was used for all tests. The diffuser length-to-diameter ratios were varied between 0.7 and 21.5, and three cylindrical ducts of different diameters were used both with and without a subsonic diffuser. An empirical method was developed to estimate the starting and operating pressure ratios of such ejector configurations using simply-determined one-dimensional normal shock relationships.

CONTENTS

	<u>Page</u>
ABSTRACT.	3
NOMENCLATURE.	7
INTRODUCTION	9
APPARATUS	10
PROCEDURE.	11
RESULTS AND DISCUSSION	
Characteristics of Ejector Starting	12
Characteristics of Ejector Minimum Cell	
Pressure Ratio	17
SUMMARY OF RESULTS	17
REFERENCES	18

TABLES

1. Description of Nozzles, Ducting, and Subsonic Diffusers.	21
2. Summary of Test Data	
a. With Subsonic Diffuser	22
b. Without Subsonic Diffuser	24

ILLUSTRATIONS

Figure

1. Typical Ejector Configurations.	25
2. Typical Nozzle Configurations	26
3. Typical Ejector Starting Phenomena for Constant Nozzle Plenum Total Pressure	27
4. Typical Effect of L/D on Ejector Starting Characteristics of Contoured Nozzles at Constant Nozzle Plenum Total Pressure	28
5. Comparison of Duct Wall Static Pressure Ratio Distribution Just Prior to Ejector Unstart with and without Subsonic Diffuser, Configs. 4a and 4as ₁ ; L/D = 9, p _{pt} = 45 psia	29

<u>Figure</u>	<u>Page</u>
6. Ejector Pressure Ratio Required for Starting; L/D \geq 8	
a. With Subsonic Diffuser.	30
b. Without Subsonic Diffuser	31
7. Effect of Diffuser Length on Ejector Perform- ance Characteristics	
a. Configurations 1a, 1a ₁ , and 1as ₁ ; p _{pt} = 45 psia . .	32
b. Configurations 3a, 3a ₁ , and 3as ₁ ; p _{pt} = 45 psia . .	33
c. Configurations 4a and 4as ₁ ; p _{pt} = 45 psia	34
d. Configurations 5a, 5a ₁ , and 5as ₁ ; p _{pt} = 45 psia . .	35
8. Variation of Starting and Operating Pressure Ratio Correction Factor with Diffuser Length-to-Diameter Ratio, L/D, for $\theta_n = 0-18$ deg	
a. With Subsonic Diffuser.	36
b. Without Subsonic Diffuser	37
9. Comparison of Estimated Starting Pressure Ratio and NASA Data (Ref. 2).	38
10. Variation of Starting and Operating Pressure Ratio Correction Factor with Diffuser Length Parameter, L/D - X/D, for $\theta_n = 0-18$ deg	
a. With Subsonic Diffuser.	39
b. Without Subsonic Diffuser	40
11. Starting and Operating Pressure Ratio Variation with Total Pressure	
a. L/D = 9.0	41
b. L/D = 1.6	42
12. Typical Cell Pressure Ratio Variation with Nozzle Plenum Total Pressure	43

NOMENCLATURE

A^*	Nozzle throat area, in. ²
A_d	Cylindrical diffuser cross-sectional area, in. ²
A_{ne}	Nozzle exit area, in. ²
D	Cylindrical diffuser diameter, in.
D^*	Nozzle throat diameter, in.
D_{ne}	Nozzle exit diameter, in.
K_1, K_1'	Ratio of experimental starting or operating pressure ratio to normal shock total pressure ratio
K_2, K_2'	Ratio of experimental starting or operating pressure ratio to normal shock static to total pressure ratio
L	Length of cylindrical supersonic diffuser measured from plane of nozzle exit, in.
L_s	Length of subsonic diffuser measured from plane of initial divergence, in.
p	Static pressure, psia
p_c	Ejector cell pressure, psia
p_{ex}	Ejector exhaust pressure, psia
p_{ne}	Nozzle exit static pressure, psia
p_{pt}	Nozzle plenum total pressure, psia
p_t	Total pressure, psia
X	Distance between nozzle exit and calculated jet impingement point, in.
γ	Ratio of specific heats
θ_n	Nozzle divergence angle at nozzle exit, deg
θ_s	Subsonic diffuser divergence angle, deg

SUBSCRIPTS

1	Upstream of normal shock
2	Downstream of normal shock

exper	Experimental
isen	Isentropic
ns	Normal shock
w	Diffuser duct wall

INTRODUCTION

The pressure altitude range within which a propulsion system may be tested in ground test facilities is normally limited by the performance of the exhaust plant. Ejectors without induced flow have therefore been developed which use the energy of the exhaust gas to reduce the pressure in the test cell to a value that allows testing at higher altitudes.

Many parameters can affect the starting and operating characteristics of ejectors without induced flow. The ratio of diffuser area to nozzle throat area, A_d/A^* , nozzle geometry, the ratio of specific heats, nozzle total pressure, diffuser length, and operation with and without a subsonic diffuser are all expected to affect these characteristics. For instance the relationship between A_d/A^* and the starting pressure ratio, p_{ex}/p_{pt} , is shown in Ref. 1 for the case of a diffuser length-to-diameter ratio (L/D) of 3 used with a subsonic diffuser. This investigation also showed that the starting pressure ratio, p_{ex}/p_{pt} , increased as the ratio of specific heats decreased. Other investigators have shown that optimum starting characteristics occur at diffuser length-to-diameter ratios between 8 and 10 when no subsonic diffuser is used (Ref. 2). Also the normal shock pressure ratios, based upon the one-dimensional isentropic Mach number for a particular ratio of diffuser to nozzle throat area, have been shown to give a satisfactory approximation of the ejector starting pressure ratio for cylindrical diffuser length-to-diameter ratios of 3 used with a subsonic diffuser (Ref. 1) and for cylindrical diffuser-plus-subsonic diffuser length-to-diameter ratios from 8 to 10 (Ref. 2). However, for diffuser lengths less than these values, the data (Ref. 2) indicate such a decrease in the starting pressure ratio, p_{ex}/p_{pt} , that the normal shock relationship cannot be used.

The length of diffuser that can be installed for a given ejector-diffuser configuration is limited in many instances because of the necessity of using existing facilities. A study was therefore made at the Rocket Test Facility (RTF), Arnold Center, Air Force Systems Command (AFSC), to determine the effect on the ejector starting and operating characteristics of varying diffuser lengths and to determine a method of estimating the starting and operating pressure ratios as a function of diffuser length and nozzle geometry. This study was Phase III of the overall study of the performance of ejectors without

induced flow. For this phase, ejector configurations with conical nozzles were selected from those used in the Phase I (Ref. 1) study, and two additional configurations having contoured nozzles with zero-deg half angles at their exit were also investigated. Diffuser length-to-diameter ratios were varied between 0.7 and 21.5, and three cylindrical ducts of different diameters were used both with and without a subsonic diffuser.

APPARATUS

Forty-two ejector configurations consisting of a conical or contoured supersonic nozzle extending into a sealed section of straight cylindrical supersonic diffuser were tested. The cylindrical diffuser exhausted into a 4-deg half-angle conical subsonic diffuser; when no subsonic diffuser was used the cylindrical diffuser exhausted into a 30-in. plenum chamber (Fig. 1).

Two of the three cylindrical supersonic diffusers tested were fabricated from standard schedule 40 steel pipe which had been machined in the region of the jet impingement point to nominal inside diameters of 6.09 and 10.19 in. A third cylindrical supersonic diffuser made of standard schedule 40 aluminum pipe having an inside diameter of 6.02 in. was also tested. The subsonic diffusers, s_2 and s_3 , were rolled from 1/4-in. and 3/8-in. thick mild steel, respectively. These two subsonic diffusers were placed together to form the subsonic diffuser designated s_1 .

All six supersonic nozzles (Fig. 2) were made of brass and were machined in one piece. The nozzles were screwed to a 3 1/2-in. -diam standard schedule 80 inlet ducting. High pressure inlet air leakage into the cell pressure region at this junction was prevented by an "O"-ring (Fig. 2). Dimensional details of these nozzles are presented in Table 1.

The configuration code designations of the nozzles, the cylindrical ducts, and the subsonic diffusers are included in Table 1. A typical ejector configuration designation would be $2cs_2$, which would mean an ejector having a 5.07 nozzle area ratio in a 10-in. diffuser with a 76-in. subsonic diffuser. The "s" designation was omitted when no subsonic diffuser was used. Each configuration was tested using various lengths of cylindrical duct, as shown in Table 2.

The following table includes the pressures measured, the range of the pressures measured, the type of measuring instrument used, and the estimated maximum error of the measured pressures. All gages were frequently calibrated against standard laboratory gages to assure that the maximum accuracy was maintained in the measurement of each parameter.

Pressure Measured	Pressure Range Measured	Measuring Instrument	Estimated Max Error
P_c	0.2 to 5 mm HgA	McLeod (with nitrogen cold trap)	-
	5 to 50 mm HgA	diaphragm-activated dial gage	± 0.2 mm HgA
P_{ex}	7 to 50 mm HgA	↓	± 0.2 mm HgA
	1 to 10 psia		± 0.04 psia
P_{pt}	1 to 46 psia		± 0.2 psia
P_{ne}	2 to 50 mm HgA	diaphragm-activated dial gage	± 0.2 mm HgA

PROCEDURE

Prior to each test the supersonic nozzle and plenum were pressure checked to insure that there was no leakage past the "O"-ring or in the instrumentation lines. After the nozzle had been installed in the test cell, the entire test cell was pressure checked, and all flanges and instrumentation fittings were sprayed with a liquid soap to permit detection of any leaks. A vacuum check was also made prior to the recording of the data as a further check on any possible leakage.

Inlet air was supplied from the RTF compressors at pressures, P_{pt} , as high as 46 psia and at temperatures approximating 100°F. The ejectors exhausted into the RTF exhaust machines which provide pressures as low as 7 mm HgA. An electrically operated throttling valve was used in the exhaust ducting to control the exhaust pressure, P_{ex} , at the exit of the ejector. The inlet supply pressure was manually controlled by a gate-type valve.

The maximum exhaust pressure at which the ejector started was obtained at constant values of p_{pt} by decreasing p_{ex} until the cell pressure, p_c , reached a minimum value. The exhaust pressure was then increased until the ejector again became unstarted (when p_c starts to increase) to determine the maximum operating exhaust pressure. This procedure was repeated at various levels of total pressure, p_{pt} .

RESULTS AND DISCUSSION

The fundamental ejector starting phenomena discussed in Ref. 3 is illustrated in Fig. 3. In the region of the performance curve marked (1), both the nozzle and the ejector were unstarted. As the ratio, p_{ex}/p_{pt} , was decreased, the nozzle became started (minimum nozzle exit pressure) at point "a" in region (2). However, the ejector did not start (minimum cell pressure) until point "b" in region (3) was reached. Point "b" occurred at the maximum starting pressure ratio. When the ratio, p_{ex}/p_{pt} , was increased after the ejector started, the reverse of the described phenomena occurred and the ejector became unstarted when the operating pressure ratio was exceeded.

To demonstrate the effect of diffuser length on the starting and operating pressure ratios, some typical data are shown in Fig. 4. For diffuser length-to-diameter ratio of 8.1, the starting and operating pressure ratios, points a and b, respectively, were essentially identical. For diffuser length-to-diameter ratios near 1.0, a significant difference existed between the starting pressure ratio, point a, and the operating pressure ratio, point b, which resulted in a significant hysteresis loop.

CHARACTERISTICS OF EJECTOR STARTING

Effect of Subsonic Diffuser

Ejector starting characteristics were determined both with and without a subsonic diffuser. Figure 5 shows the static pressure distribution in a long cylindrical diffuser ($L/D = 9$) at values of p_{ex}/p_{pt} slightly less than the operating pressure ratio. This wall static pressure distribution in the cylindrical diffuser remained the same, whether a subsonic diffuser was or was not used. The subsonic diffuser gave a slight increase in pressure recovery which

resulted in an increased ejector starting pressure ratio although the major portion of the pressure rise occurred in the cylindrical diffuser section.

The experimental starting and operating pressure ratio was improved approximately 12 to 18 percent for long diffusers ($L/D > 8$) when a subsonic diffuser was used (Figs. 6 and 7). As diffuser length was decreased ($L/D < 8$), the subsonic diffuser was found to improve the starting pressure ratio from 10 to 68 percent (Fig. 7).

The improvement in starting pressure ratio produced by the subsonic diffuser can be very closely predicted for long diffusers by comparing the one-dimensional relationships for static-to-total and total-to-total pressure ratios across a normal shock. For a given cylindrical duct to nozzle throat area ratio, A_d/A^* , a one-dimensional isentropic Mach number was determined. Then the corresponding normal shock static-to-total pressure ratio which occurred when no subsonic diffuser was used (Fig. 6b) was compared with the total pressure ratio across a normal shock which occurred when a subsonic diffuser was used (Fig. 6a). This theoretical comparison predicted an approximate 12 to 15-percent improvement in the starting pressure ratio when a subsonic diffuser was used.

Effect of Supersonic Diffuser Length

The starting pressure ratio reached a maximum at diffuser length-to-diameter ratios of 3 for ejectors equipped with a subsonic diffuser and a conical nozzle (Figs. 7a through c). It is also significant that the starting pressure ratio equaled the operating pressure ratio above a $L/D = 3$ for conical nozzles. For the contoured nozzles the starting pressure ratio reached a maximum at an approximate $L/D = 8$ (Fig. 7d). It was noted that a small difference existed between the starting and operating pressure ratios at $L/D > 8$ for the contoured nozzles.

As the length of the cylindrical supersonic diffuser section was decreased below the optimum values of L/D , the starting pressure ratios also decreased (Fig. 7), although the rate of decrease was less for configurations having the contoured nozzles than for the conical nozzles. No significant change in the operating pressure ratio was noted for diffuser lengths as low as $L/D = 1.6$ for ejectors equipped with conical nozzles and a subsonic diffuser (Figs. 7a through c). The ejectors equipped with the contoured nozzles, however, had a decreasing operating pressure ratio below approximately $L/D = 8$ (Fig. 7d). Figure 7 also shows that the difference between the starting and operating pressure ratios (the ejector hysteresis) increased as the L/D was decreased.

When no subsonic diffuser was used, the optimum L/D for conical nozzles increased to approximately 5. For contoured nozzles no major change was indicated in the optimum L/D when no subsonic diffuser was used; however insufficient data were obtained to evaluate this adequately. There was no variation in the starting pressure ratio for diffuser lengths above these optimum values except for a slight decrease in p_{ex}/p_{pt} resulting from the frictional effects of very long diffusers.

As the length of the cylindrical supersonic diffuser section was decreased below the optimum values of L/D when no subsonic diffuser was used, the starting hysteresis was noticeably increased for the conical nozzles as compared with that obtained using a subsonic diffuser (Figs. 7a through c).

Estimating Ejector Starting and Operating Performance

Although the compression shock system in a long duct is a series of lambda shocks resulting from an interaction between the boundary shock and the boundary layer on the duct walls, Shapiro (Ref. 4) states that one-dimensional normal shock relationship used with the duct inlet Mach number will predict the pressure rise across the shock system within approximately 6 percent. This good agreement is explained by the fact that the wall shearing forces in the region of separation caused by shock-boundary layer interaction are extremely small. Although Shapiro's results were obtained for uniform duct inlet flow, the experimental results for ejectors in which the flow was not expected to be uniform still showed good agreement with one-dimensional normal shock relationships.

As shown in Fig. 6, the experimental results for diffuser length-to-diameter ratios equal to or greater than 8 were approximately 88 percent of the theoretical normal shock values $(p_2/p_1)_{ns}$ for conical and contoured nozzles when a subsonic diffuser was used. When no subsonic diffuser was used, the experimental results were approximately 90 percent of the theoretical normal shock values $(p_2/p_1)_{ns}$ for conical nozzles and 80 percent of those for contoured nozzles.

A more accurate prediction of the starting and operating pressure ratios can be obtained by correcting the theoretical normal shock value by a parameter which is a function of nozzle geometry and the diffuser length-to-diameter ratio. This correction parameter is expressed as a ratio of the experimental starting or operating pressure ratios to the theoretical normal shock value.

For ejectors having subsonic diffusers which essentially diffuse the air to a zero velocity condition, the total pressure recovery across a normal shock for the one-dimensional isentropic Mach number corresponding to the area ratio of the cylindrical diffuser in the region of jet impingement to the nozzle throat area, A_d/A^* , was used. Thus,

$$K_1 = (P_{ex}/P_{P_t})_{\text{exper}} / (P_{t_2}/P_{t_1})_{ns} \quad (1)$$

For ejectors having no subsonic diffuser, it was assumed that the ejector system diffused to the exhaust conditions by the static to total pressure ratio across a normal shock for the isentropic Mach number corresponding to A_d/A^* . Thus,

$$K_2 = (P_{ex}/P_{P_t})_{\text{exper}} / (P_0/P_{t_1})_{ns} \quad (2)$$

The correction constant was calculated for each test configuration and was plotted vs the diffuser length-to-diameter ratio, L/D (Figs. 8a and b). For diffuser lengths above optimum there was a small change in the correction constants with increasing diffuser length, which varied primarily as a function of nozzle geometry and whether or not a subsonic diffuser was used. Below the optimum L/D the correction factor also varied considerably as a function of whether or not a subsonic diffuser was used. The decrease in K_2 for diffusers having $L/D > 10$ (Fig. 8b) reflected the pressure loss resulting from frictional effects discussed in Ref. 4.

For configurations having diffuser lengths greater than optimum and either contoured or conical nozzles, the values of the correction constants varied less than ± 5 percent at any given length for all configurations tested. For diffuser lengths less than optimum, this variation increased to ± 10 percent (Figs. 8a and b). Using the values of K from Fig. 8, the starting pressure ratios from Ref. 2 can be estimated within ± 10 percent for diffuser length-to-diameter ratios greater than 4 (Fig. 9). Although the described method predicts the starting pressure ratio for ejector configurations using nozzle shapes similar to those tested, its use for ejectors having nozzles with other shapes may require modifications to the presented methods.

As diffuser length approaches the jet impingement distance, the diffuser length parameter, $L/D - X/D$, would provide a better correlation parameter than L/D . This would appear to be a more realistic approach since it more nearly reflects the effective length of duct as far as the pressure recovery phenomena in the diffuser are concerned. Figures 10a and b show an improvement in correlation of as much as 15 percent for some configurations equipped with short diffusers when this parameter was used. However, as the diffuser L/D approaches X/D the values of K_1' and K_2' are expected to become unreliable

because the minimum cell pressure ratio may change and thus shift the region of jet impingement. The following jet impingement distances were used in determining the length parameter for the experimental data plotted in Fig. 10:

A/A*	D = 6.00 in.		D = 10.19 in.	
	X	X/D	X	X/D
3.63	2.05	.336	4.7	.462
5.07	2.14	.351	5.0	.492
10.85	2.3	.378	6.46	.633
25.00	3.85	.632	8.8	.863
23.68	3.19	.513	-	-

These impingement distances were calculated using Latvala's procedure (Ref. 6) for a total pressure of 45 psia and the experimental minimum cell pressure ratio, p_c/p_{pt} (which can be calculated using Ref. 5).

Total Pressure Effect

The ejector starting and operating characteristics remained unchanged by a variation in nozzle plenum total pressure in the case of an L/D equal to 9, as shown in Fig. 11a. However, as diffuser length was decreased to values at which the jet impingement distance became an important parameter, the ejector starting and operating pressure ratios varied with total pressure level, as shown in Fig. 11b. This variation is in order since jet impingement distance is a function of minimum cell pressure ratio which is also a function of nozzle total pressure. Figure 12 shows a typical variation in the minimum cell pressure ratio, p_c/p_{pt} , with total pressure. Jet impingement studies which have been made (Refs. 6 and 7) show that as the cell pressure ratio increases, the jet impingement distance increases. This gives the decrease in the length parameter term, $L/D - X/D$, in Fig. 10 and a corresponding decrease in the value of "K", which results in a decrease in the starting or operating pressure ratio for short diffuser lengths. Thus, the influence of total pressure level in the case of very short diffusers ($L/D \leq 3$) indicates that the accuracy with which the starting and operating pressure ratios can be predicted will depend upon how accurately the jet impingement distance can be calculated. Reference 5 presents a good method of estimating the cell pressure for a given configuration: it can be used in determining the impingement distance.

CHARACTERISTICS OF EJECTOR MINIMUM CELL PRESSURE RATIO

The effect of diffuser length on ejector minimum cell pressure ratio, p_c/p_{pt} , is shown in Figs. 7a through d. The cell pressure ratio varied only slightly as a result of diffuser length or the method of subsonic diffusion. The experimental results show that the minimum cell pressure ratio was not affected appreciably at diffuser lengths as low as $L/D = 0.7$. It is believed that the cell pressure ratio would not be affected at diffuser lengths shorter than this, provided the diffuser length was maintained greater than the impingement distance.

SUMMARY OF RESULTS

An investigation of ejectors without induced flow was made to determine the effects of varying diffuser lengths on ejector performance. The results of this investigation may be summarized as follows:

1. An optimum length of cylindrical diffuser for an ejector without induced flow was determined for which the starting and operating pressure ratios are a maximum. For lengths greater than optimum, the starting and operating pressure ratios remained constant except for a slight decrease resulting from friction effects in the long duct. This optimum length was found to be a function of nozzle geometry and type of subsonic diffusion. The optimum diffuser length-to-diameter ratios were approximately 3 for the 18-deg conical nozzles and approximately 8 for the zero-deg exit angle contoured nozzle when a subsonic diffuser was used. When no subsonic diffuser was used, the optimum length-to-diameter ratios were approximately 5 for the 18-deg conical nozzles and approximately 9 for the zero-deg contoured nozzle.
2. The essentially constant ejector starting and operating pressure ratios for diffuser length-to-diameter ratios greater than the optimum length can be estimated within 10 to 20 percent by using a simple one-dimensional normal shock relationship. The starting pressure ratio for these diffuser lengths was found to be a function of nozzle geometry, the ratio of duct-to-nozzle throat area, the ratio of specific heat, and the type of subsonic diffusion.

3. For diffuser lengths less than optimum, the starting pressure ratio decreased, and a hysteresis separated the starting and operating pressure ratios. The starting characteristics became a function of an additional parameter, impingement distance, at diffuser lengths less than optimum.
4. The minimum cell pressure was not affected by diffuser length above lengths only slightly greater than the jet impingement distance.
5. The subsonic diffuser improved the maximum ejector starting pressure ratio from 12 to 18 percent for diffuser length-to-diameter ratios greater than 8 by decreasing the total pressure losses of the flow leaving the cylindrical diffuser. At length-to-diameter ratios less than 8, the subsonic diffuser improved the starting characteristics from approximately 10 to 68 percent.
6. An empirical method was developed which can be used to estimate the starting and operating pressure ratios for ejector configurations having 18-deg conical or zero-deg exit angle contoured nozzles located in a cylindrical duct.

REFERENCES

1. Barton, D. L. and Taylor, D. "An Investigation of Ejectors without Induced Flow, Phase I." AEDC-TN-59-145, December 1959.
2. Jones, W. L., Price, H. G., Jr., and Lorenzo, C. F. "Experimental Study of Zero-Flow Ejectors Using Gaseous Nitrogen." NASA-TN-D-203, March 1960.
3. Emmons, H. W. Fundamentals of Gas Dynamics, Vol. III. Princeton University Press, 1954.
4. Shapiro, A. H. The Dynamics and Thermodynamics of Compressible Fluid Flow, Vol. I. The Ronald Press Company, New York, 1953.
5. Bauer, R. C. and German, R. C. "Some Reynolds Number Effects on the Performance of Ejectors without Induced Flow." AEDC-TN-61-87, August 1961.

6. Latvala, E. K. "Spreading of Rocket Exhaust Jets at High Altitude." AEDC-TR-59-11, June 1959.
7. Bauer, R. C. and Schlumpf, R. L. "Experimental Investigation of Free Jet Impingement on a Flat Plate." AEDC-TN-60-223, March 1961.

TABLE I
DESCRIPTION OF NOZZLES, DUCTING, AND SUBSONIC DIFFUSERS

Nozzle Config.	Nozzle Dimensions				Duct Config. a		Duct Config. a1		Duct Config. c	
	A_{ne}/A^*	D^* in.	D_{ne} in.	θ_n deg	D in.	A_d/A^*	D in.	A_d/A^*	D in.	A_d/A^*
1	3.53	2.200	4.190	18	6.09	7.7	6.02	7.5	10.19	21.5
2	5.07	1.852	4.170	18		10.8		10.8		30.3
3	10.85	1.262	4.155	18		23.3		22.6		65.3
4	25.00	0.831	4.155	18		53.7		52.5		150.4
5	23.68	0.900	4.380	0		45.8		44.7		128.2
6	100.00	0.442	4.420	0	6.09	189.8	6.02	185.0	10.19	531.4
Tolerance		± 0.001	± 0.001		± 0.01		± 0.01		± 0.01	

Subsonic Diffuser	L_s in.	θ_s deg	Inlet Diam. in.	Exit Diam. in.	L_s/D
S1	97	4	6.08	20.0	15.9
S2	76	4	10.13	20.0	7.5
S3	16	4	6.09	10.19	2.6
Tolerance	± 0.25		± 0.01	± 0.01	

TABLE 2
SUMMARY OF TEST DATA
a. With Subsonic Diffuser

Config.	A_{nc}/A^*	A_d/A^*	L/D	Ppt psia	P_c/P_{pt}	P_{nc}/P_{pt}	P_{ex}/P_{pt} (Oper.)	P_{ex}/P_{pt} (Start)
1as ₁	3.63	7.7	1.6	5.2	.0164	.0355	.1656	.1348
				10.0	.0131	.0323	.1680	.1430
				15.6	.0106	.0317	.1687	.1463
				21.1	.00925	.0318	.1694	.1508
				25.8	.008475	.0320	.1686	.1524
				31.3	.00915	-	.1693	.1483
				38.2	.0102	-	.1675	.1425
			1.6	45.0	.0103	.0323	.1685	.130
			3.0*	38.7	.00992	-	.1674	.1674
			6.0	45.0	.0106	.0311	.158	.158
			9.0	5.2	.01645	.0308	.1646	.1646
				10.4	.0133	.0312	.167	.167
				15.5	.01126	.031	.165	.165
				21.0	.00957	.031	.164	.164
				25.9	.00861	.0309	.1645	.1645
				31.2	.00835	.0309	.165	.165
				40.0	.00832	-	.1653	.1653
				40.6	.0100	-	.1656	.1656
1as ₂	3.63	7.7	9.0	45.0	.0106	.0308	.1656	.1656
2as ₁	5.07	10.8	3.0*	37.0	.00558	-	.1225	.1225
			6.0	45.0	.00553	.0215	.1155	.1155
			9.0	45.0	.00553	.0215	.1214	.1214
3as ₁	10.85	23.3	1.6	8.9	.00391	-	-	-
				14.4	.00391	.00596	.0473	.0377
				20.3	.00392	.00587	.0504	.0388
				25.2	.00268	.00580	.0544	.0417
				29.9	.00266	.00583	.0576	.0459
				35.0	.00199	.00595	.0562	.0435
				39.4	.00184	.00595	.0562	.0406
				44.3	.00177	.00590	.0562	.0406
			1.6	45.0	.00177	.0059	.057	.041
			3.0*	45.5	.00181	-	.0599	.0599
			6.0	45.0	.00177	.00558	.057	.057
			9.0	5.0	.00466	.00522	.060	.060
				9.7	.00399	.00588	.0604	.0604
				15.0	.00404	.00498	.0604	.0604
				20.0	.00389	.00517	.0610	.0610
				30.0	.00243	.00539	-	-
				34.9	.00203	.00556	.060	.060
				40.5	.00182	.0056	.0598	.0598
3as	10.85	23.3	9.0	45.0	.00175	.0056	.0598	.0598
3as	10.85	23.3	5.5	45.0	.00175	.00584	.0566	.0552

*Data from tests reported in Ref. 1

TABLE 2 (Continued)

a. Concluded

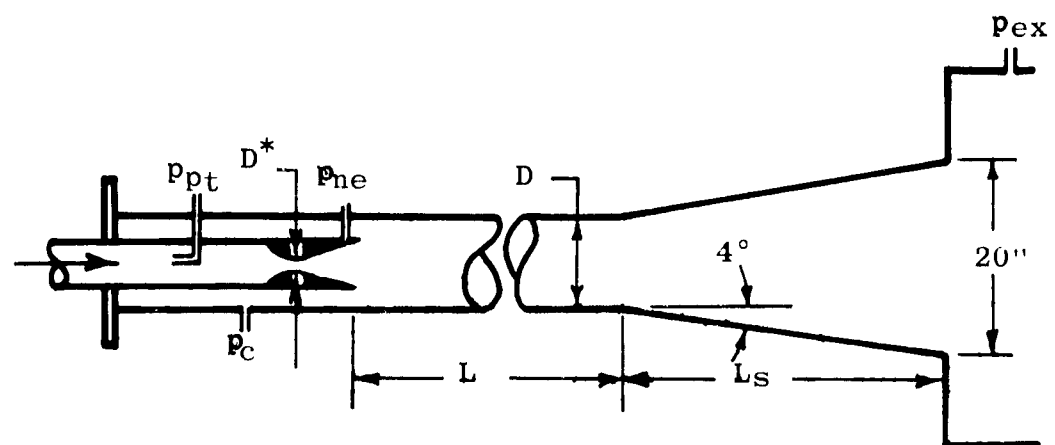
Config.	A_{ne}/A^*	A_d/A^*	L/D	Ppt psia	P_c/P_{pt}	P_{ne}/P_{pt}	P_{ex}/P_{pt} (Oper.)	P_{ex}/P_{pt} (Start)
4as ₁	25.00	53.7	1.6	16.0	.00143	-	-	-
↓	↓	↓	↓	21.0	.00136	.00166	.0192	.0136
↓	↓	↓	↓	24.9	.00134	.00148	.0209	.0145
↓	↓	↓	↓	29.7	.00126	.00137	.0222	.0165
↓	↓	↓	↓	34.8	.00107	.00133	.0241	.0178
↓	↓	↓	↓	39.7	.00094	.00129	.0240	.0175
↓	↓	↓	↓	44.2	.00088	.00129	.0249	.0166
↓	↓	↓	1.6	45.0	.00087	.0013	.025	.0163
↓	↓	↓	3.0*	44.3	.00097	-	.0256	.0256
↓	↓	↓	6.0	45.0	.00098	.00114	.0255	.0255
↓	↓	↓	9.0	14.8	.00134	-	.0269	.0269
↓	↓	↓	↓	19.8	.00137	.00083	.0267	.0267
↓	↓	↓	↓	24.9	.00126	.000972	.0265	.0265
↓	↓	↓	↓	34.8	.00111	.000917	.0266	.0266
↓	↓	↓	↓	45.0	.00095	.0011	.0267	.0267
4as ₁	25.00	53.7	9.0	45.5	.000936	.00111	.0268	.0268
4as ₁	25.00	53.7	5.5	45.0	.00098	.00114	.0246	.0241
5as ₁	23.68	45.8	0.7	45.0	.00029	.0037	.0105	.0085
↓	↓	↓	5.2	↓	.00031	.00353	.0256	.0215
↓	↓	↓	8.1	↓	.00032	.0035	.030	-
5as ₁	↓	↓	4.7	↓	.00031	.00382	.0205	.0132
6as ₁	100	189.8	8.1	↓	-	-	.00728	-
1cs	3.63	21.5	3.0*	↓	.0026	-	.0607	.0607
↓	↓	↓	6.0	↓	.0027	.0308	.0607	.0607
↓	↓	↓	9.0	↓	.0027	-	.0603	.0603
2cs	5.07	30.3	3.0*	↓	.001616	-	.0444	.0444
↓	↓	↓	6.0	↓	.001518	-	.0438	.0438
↓	↓	↓	9.0	↓	.001568	-	.0437	.0437
3cs	10.85	65.3	3.0*	↓	.00056	-	.0222	.0222
↓	↓	↓	6.0	↓	.00056	-	.0218	.0218
4cs	25.0	150.4	3.0*	↓	.000268	-	.00983	.00983
↓	↓	↓	6.0	↓	.000275	.001	.00969	.00969
↓	↓	↓	9.0	45.0	.000268	-	.00954	.00954

*Data from tests reported in Ref. 1

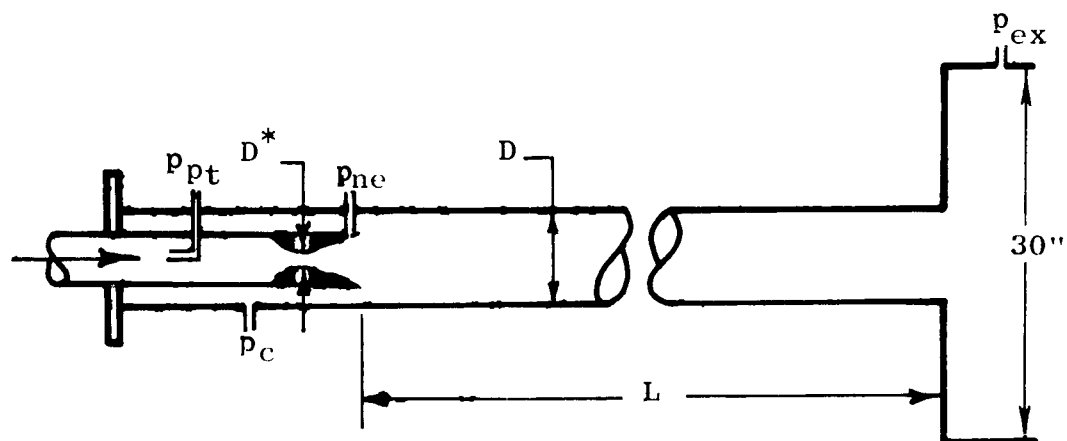
TABLE 2 (Concluded)
b. Without Subsonic Diffuser

Config.	A_{nt}/A^*	A_d/A^*	L/D	P_{pt} psia	P_c/P_{pt}	P_{ne}/P_{pt}	P_{ex}/P_{pt} (Oper.)	P_{ex}/P_{pt} (Start)
1a	3.63	7.7	1.6	45.0	.0106	.0303	.1396	.0867
↓	↓	↓	3.0	↓	.0106	.0308	.144	.1222
3a	10.85	23.3	1.6	↓	.00173	.0058	.051	.022
↓	↓	↓	3.0	↓	.00175	.0058	.0525	.0335
4a	25.00	53.7	1.6	↓	.000915	-	.022	.0091
↓	↓	↓	3.0	↓	.00097	.00125	.023	.0158
↓	↓	↓	9.0	↓	.0010	.00096	.0228	.0228
↓	↓	↓	21.5	↓	-	.00115	.0224	.0224
5a	23.68	45.8	0.7	↓	.00030	.0037	-**	.00268
↓	↓	↓	2.3	↓	.00031	.00365	.0094	.00295
↓	↓	↓	8.1	↓	.00033	.00345	.0247	-
↓	↓	↓	20.5	↓	.00036	.00355	.0245	-
6a	100	189.8	20.5	↓	-	.00094	.0061	.006
1a ₁	3.63	7.5	9.1	↓	.0106	.0328	.148	.148
3a ₁	10.85	22.8	↓	↓	.00195	.0059	.054	.054
4a ₁	25.00	52.5	↓	↓	.00106	-	.0242	.0242
5a ₁	23.68	44.7	9.1	45.0	.000345	.00352	.0264	.0242

**Instability of ejector starting performance prevented the operating pressure from being determined.



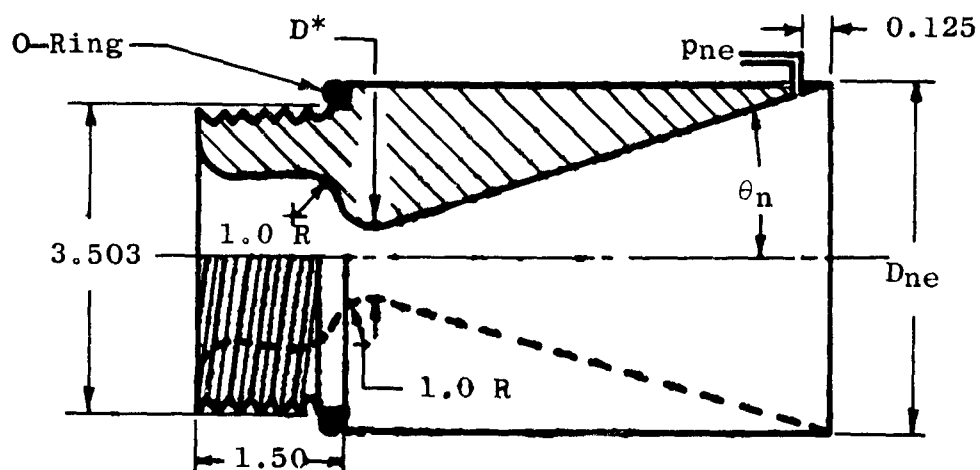
a. With Subsonic Diffuser



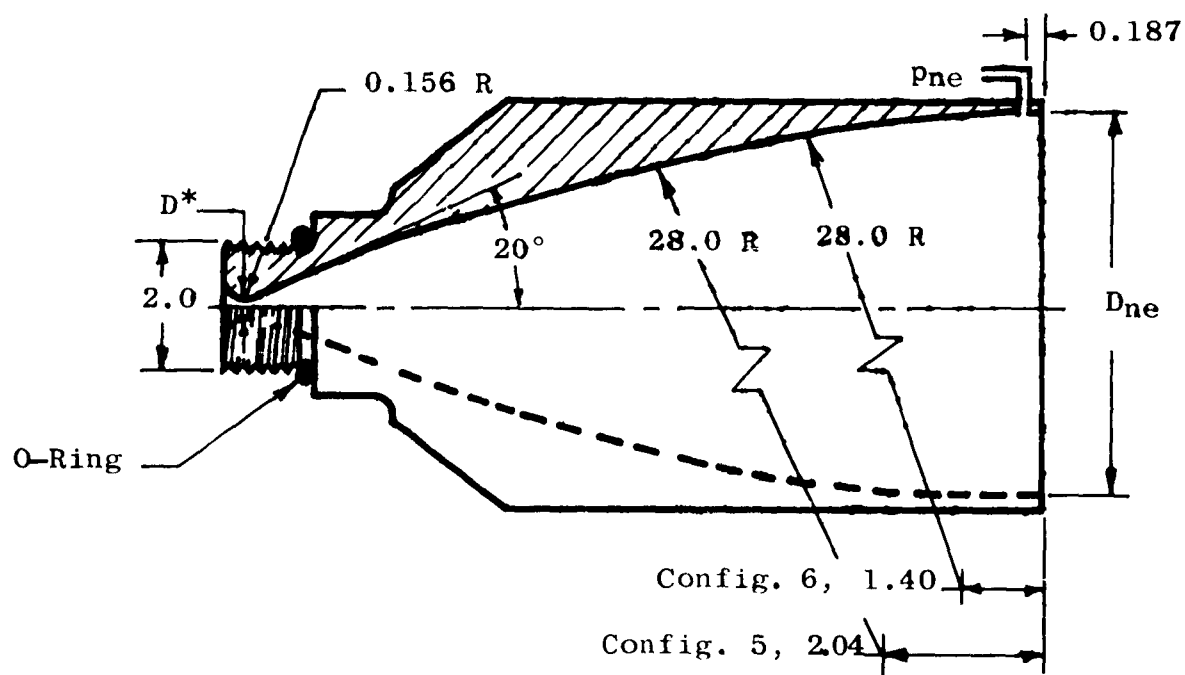
b. Without Subsonic Diffuser

Fig. 1 Typical Ejector Configurations

All dimensions
are in inches.



a. Conical Nozzle Detail



b. Contoured Nozzle Detail

Fig. 2 Typical Nozzle Configurations

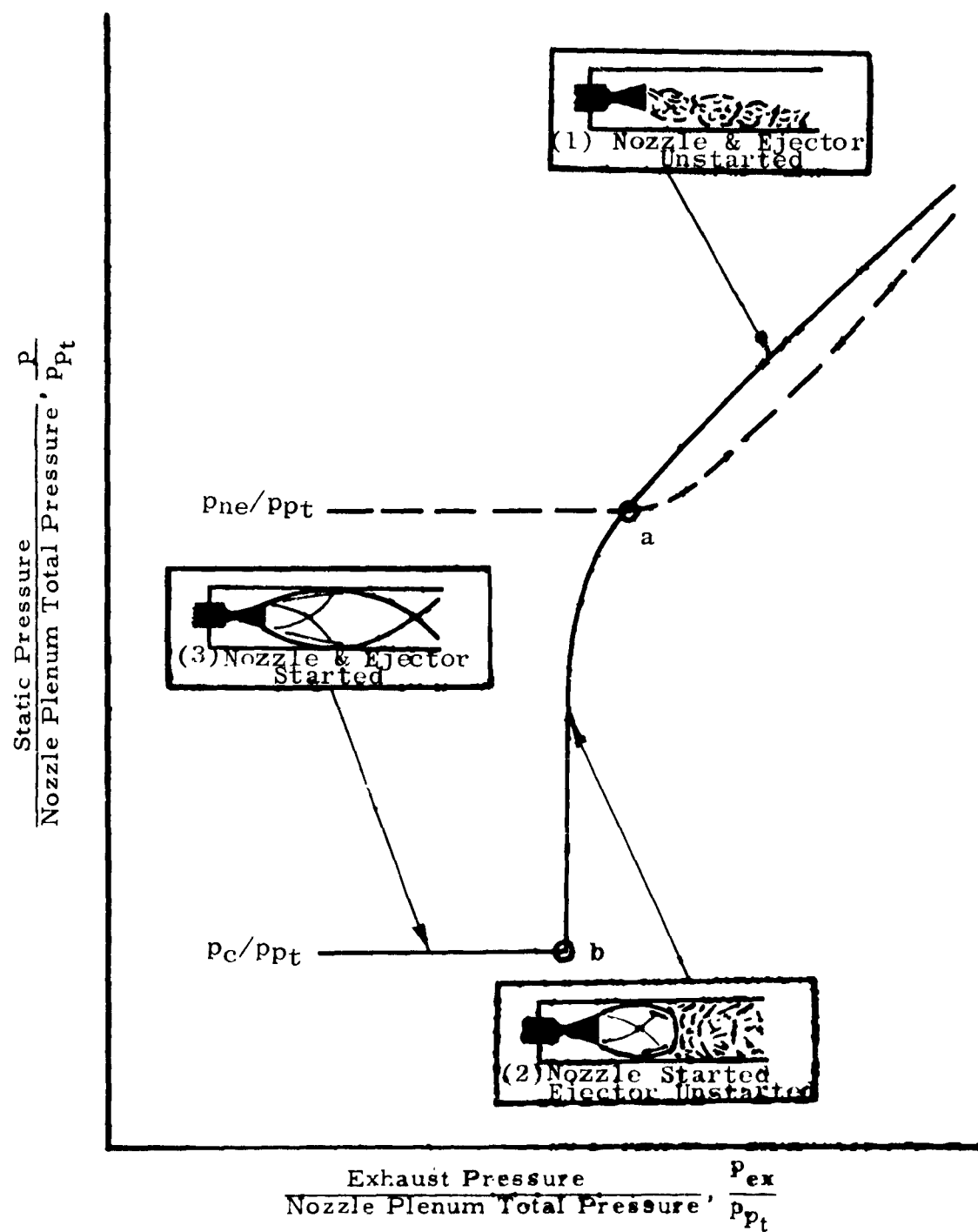


Fig. 3 Typical Ejector Starting Phenomena for Constant Nozzle Plenum Total Pressure

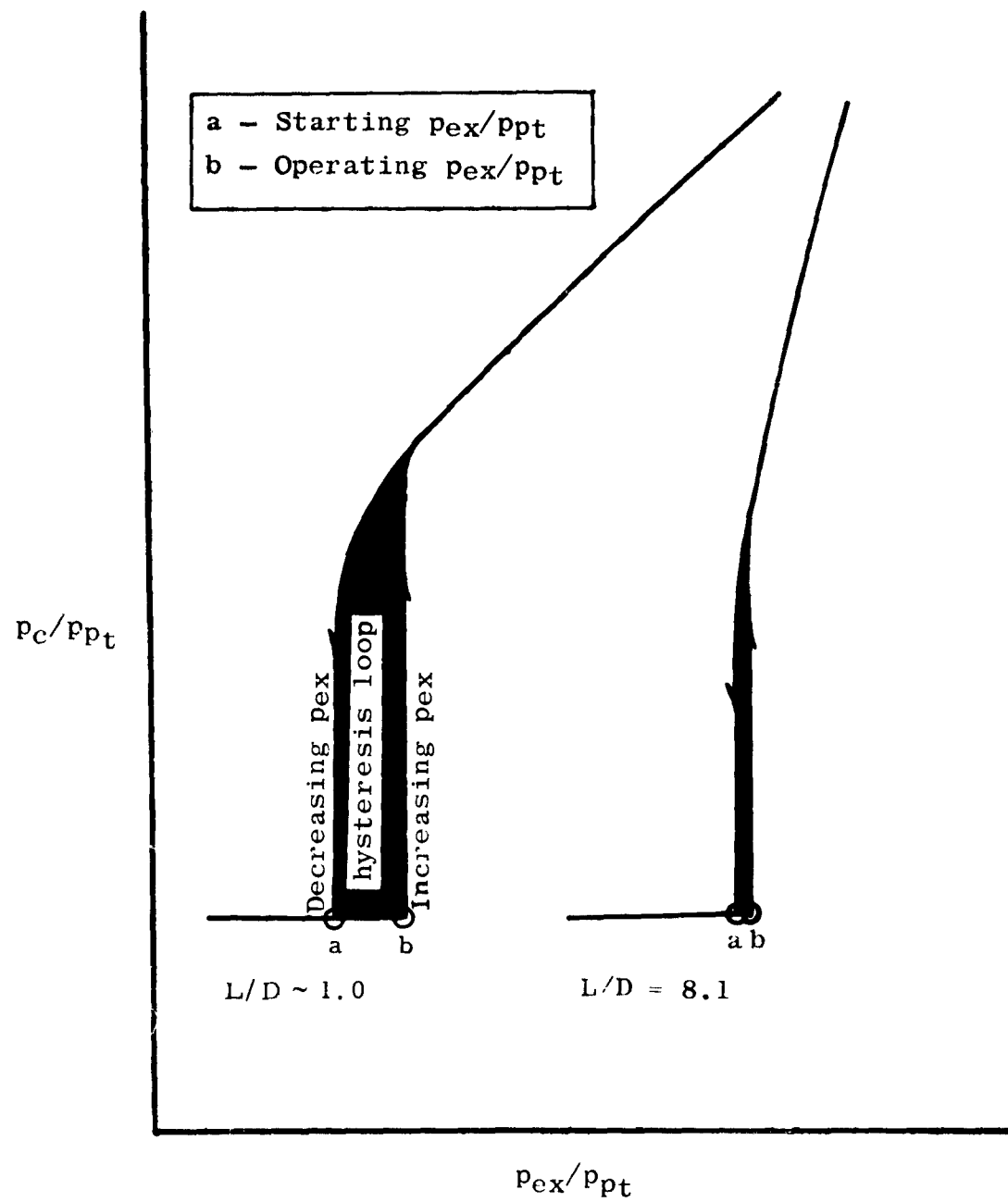


Fig. 4 Typical Effect of L/D on Ejector Starting Characteristics of Contoured Nozzles at Constant Nozzle Plenum Total Pressure

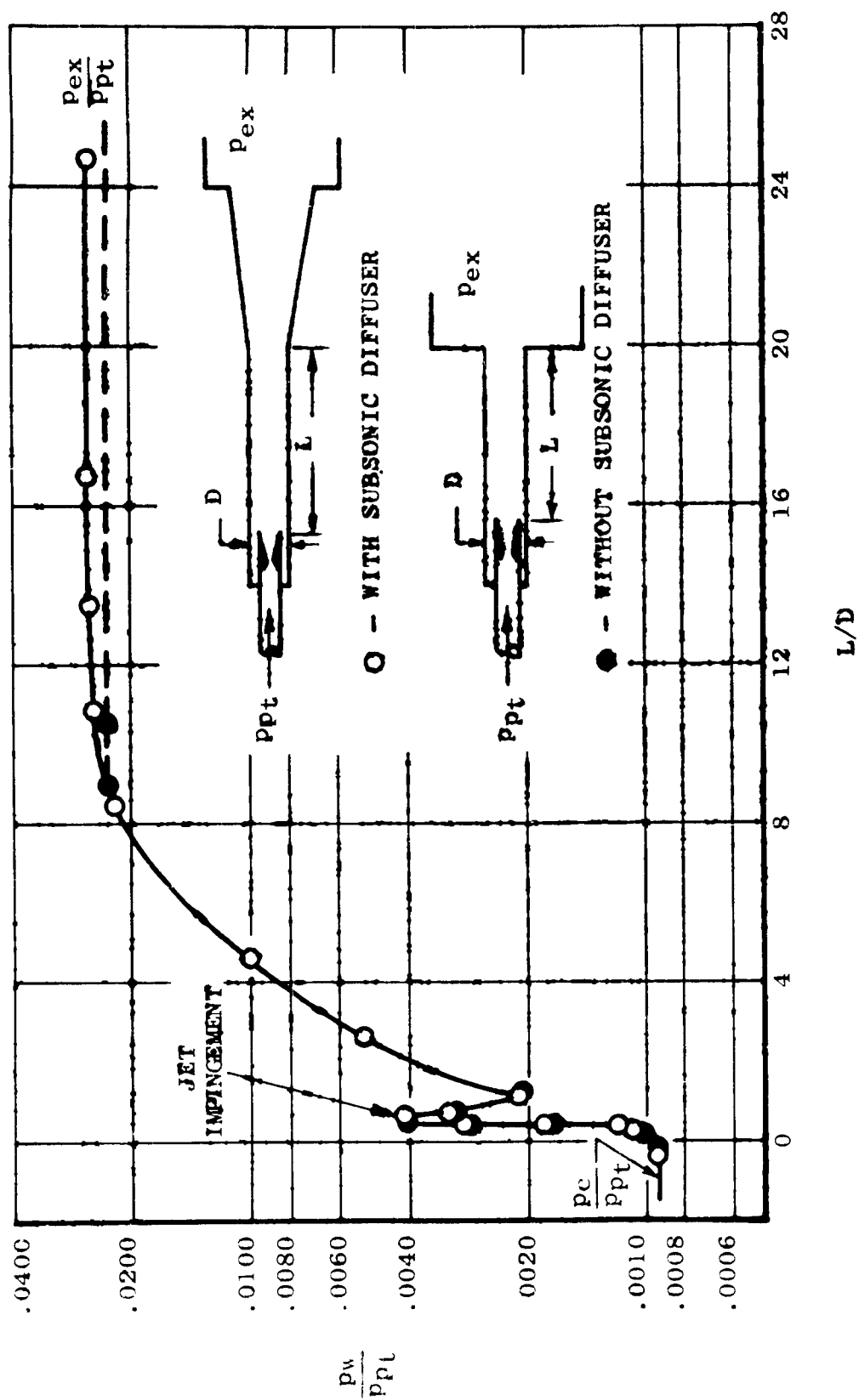
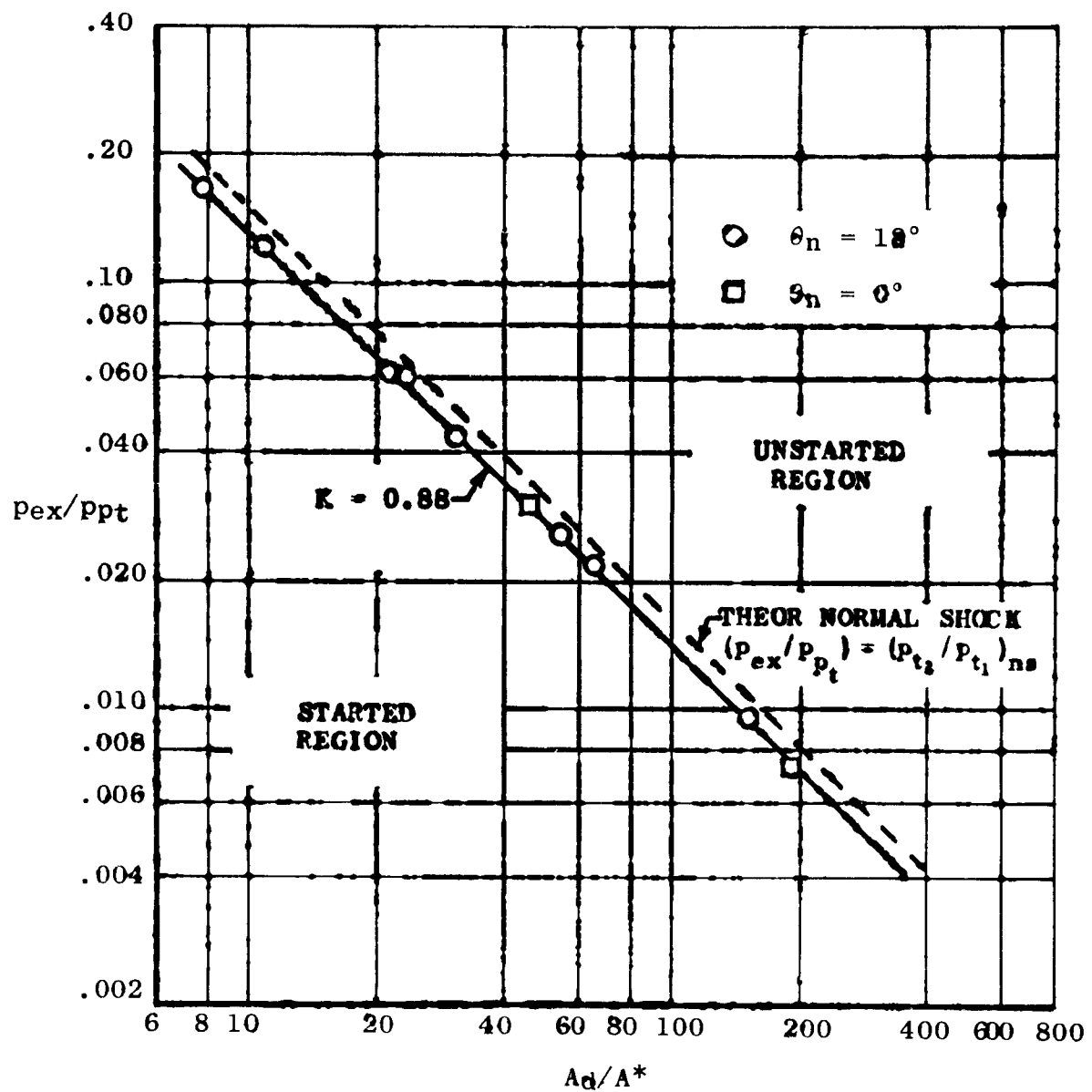
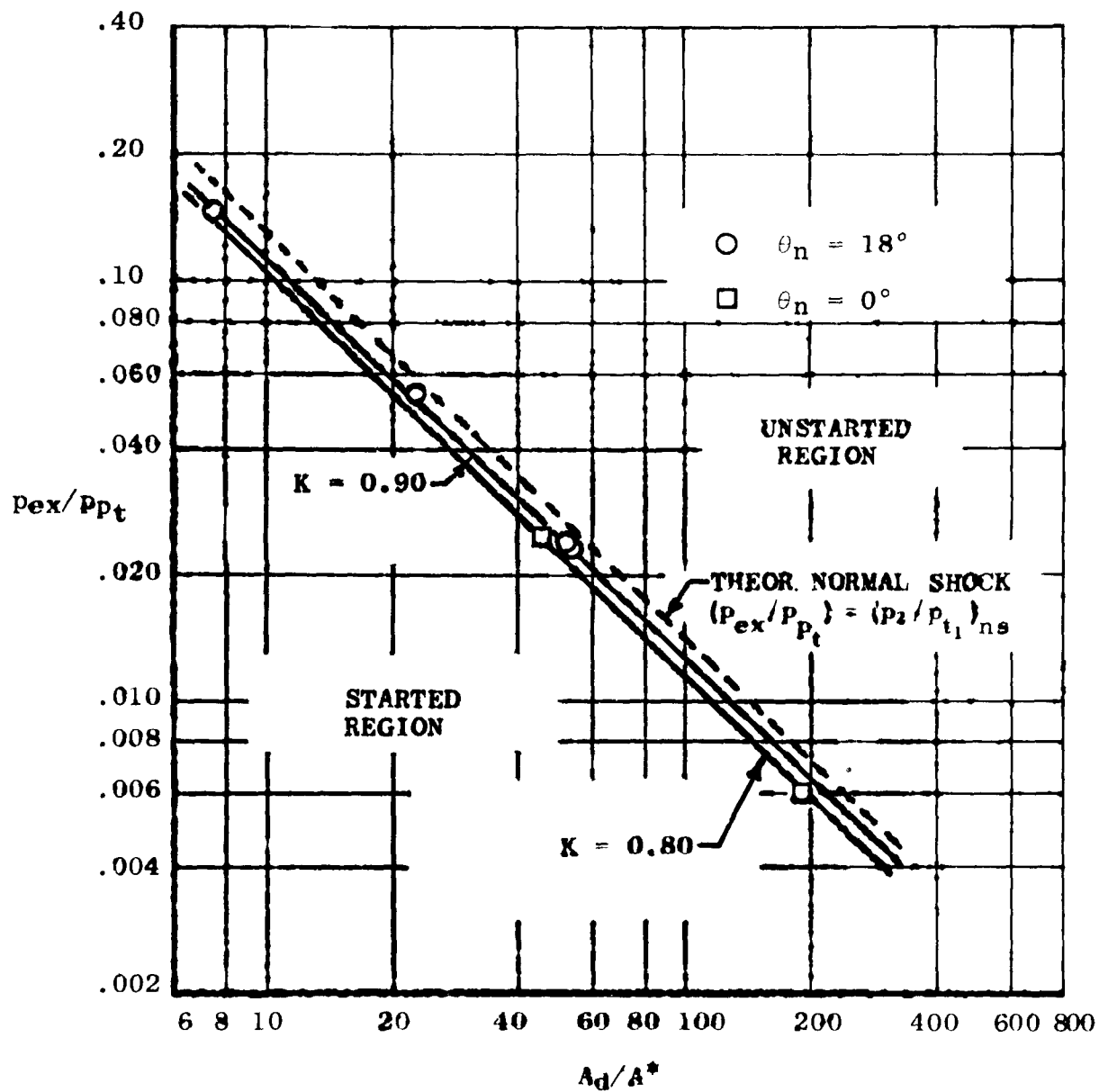


Fig. 5 Comparison of Duct Wall Static Pressure Ratio Distribution Just Prior to Ejector Unstart with and without Subsonic Diffuser, Configs. 4a and 4a1; $L/D = 9$, $p_{pt} = 45$ psia



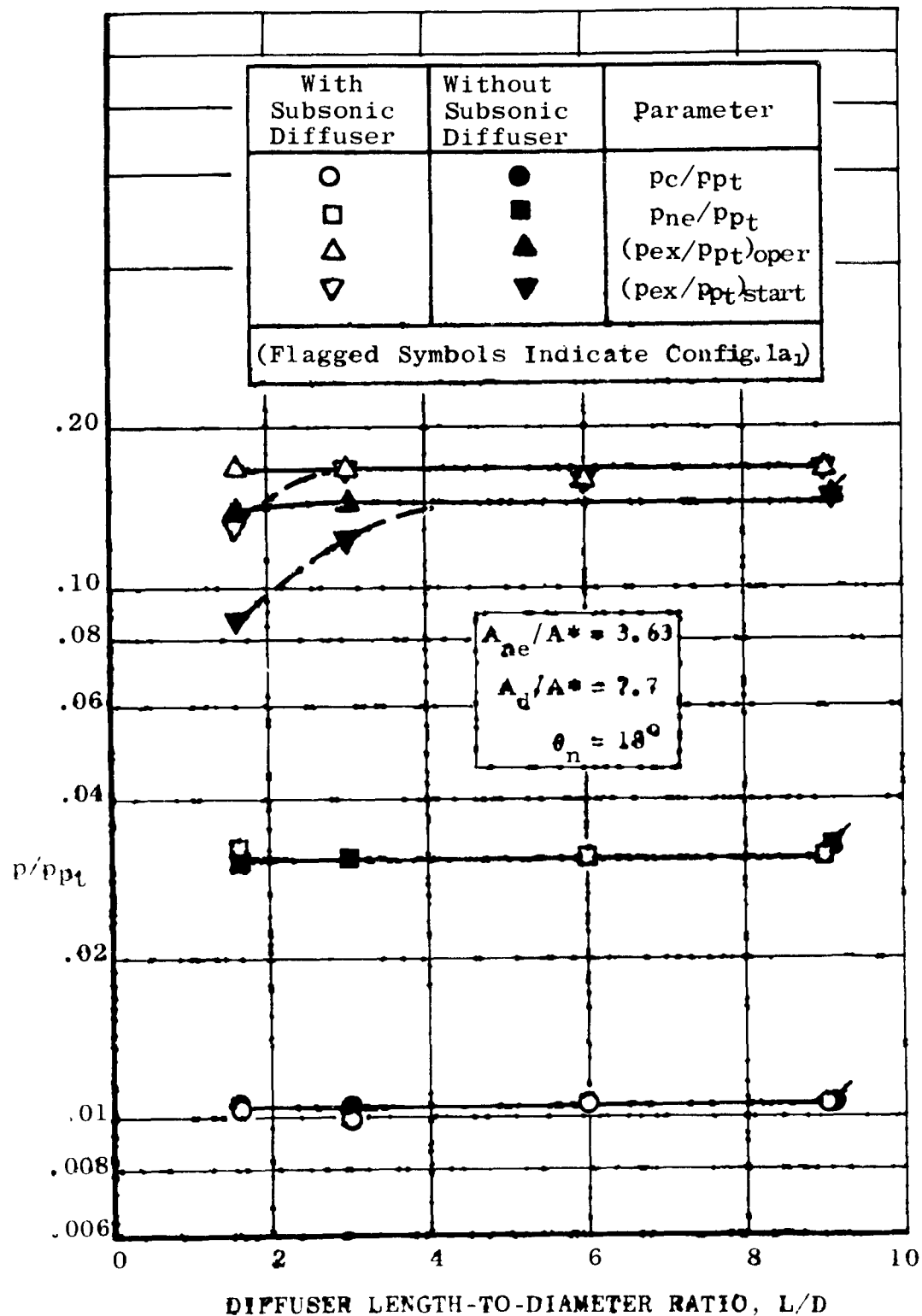
a. With Subsonic Diffuser

Fig. 6 Ejector Pressure Ratio Required for Starting; $L/D \geq 8$



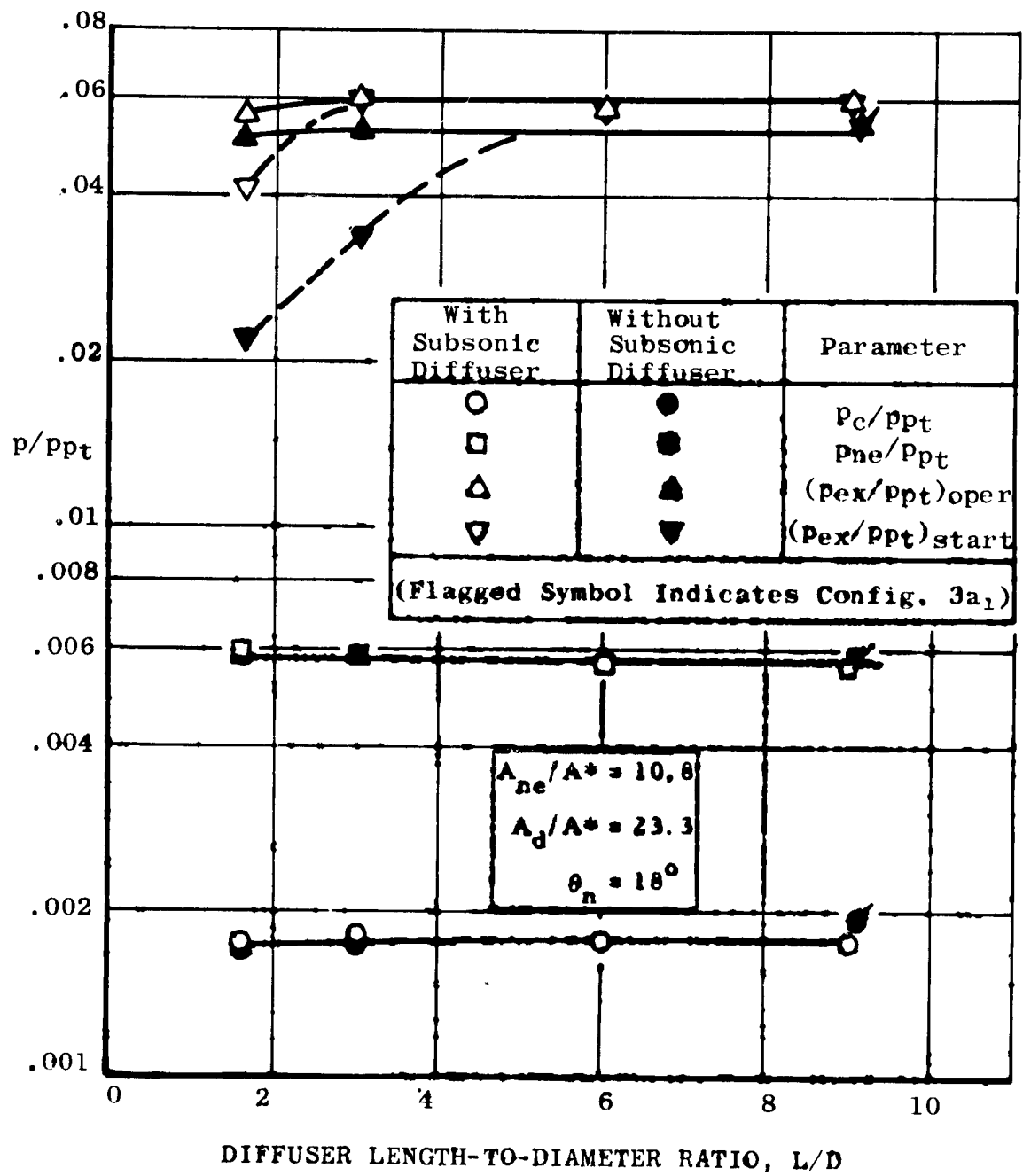
b. Without Subsonic Diffuser

Fig. 6 Concluded



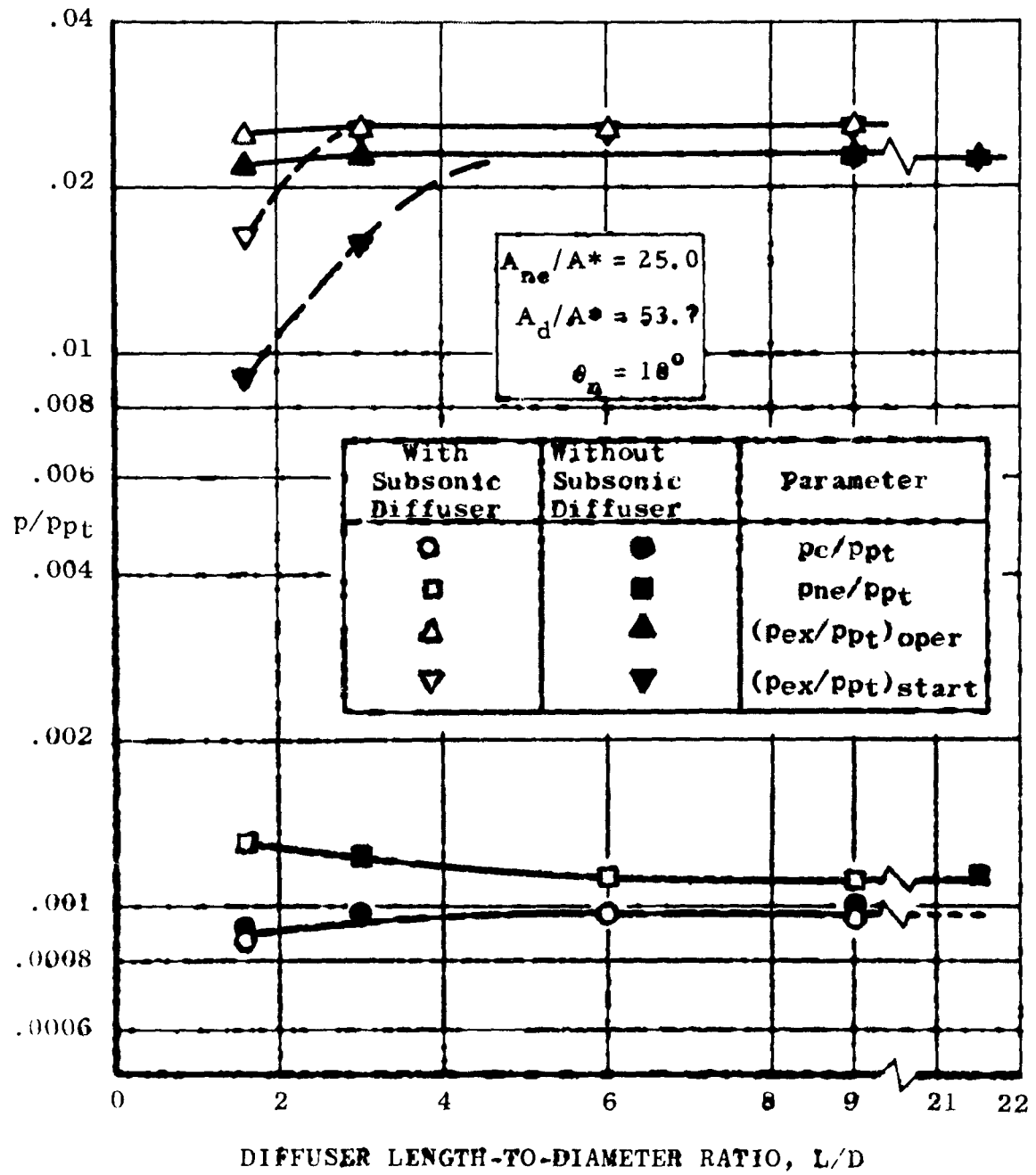
a. Configurations 1a, 1a₁, and 1a₁; $p_{pt} = 45$ psia

Fig. 7 Effect of Diffuser Length on Ejector Performance Characteristics



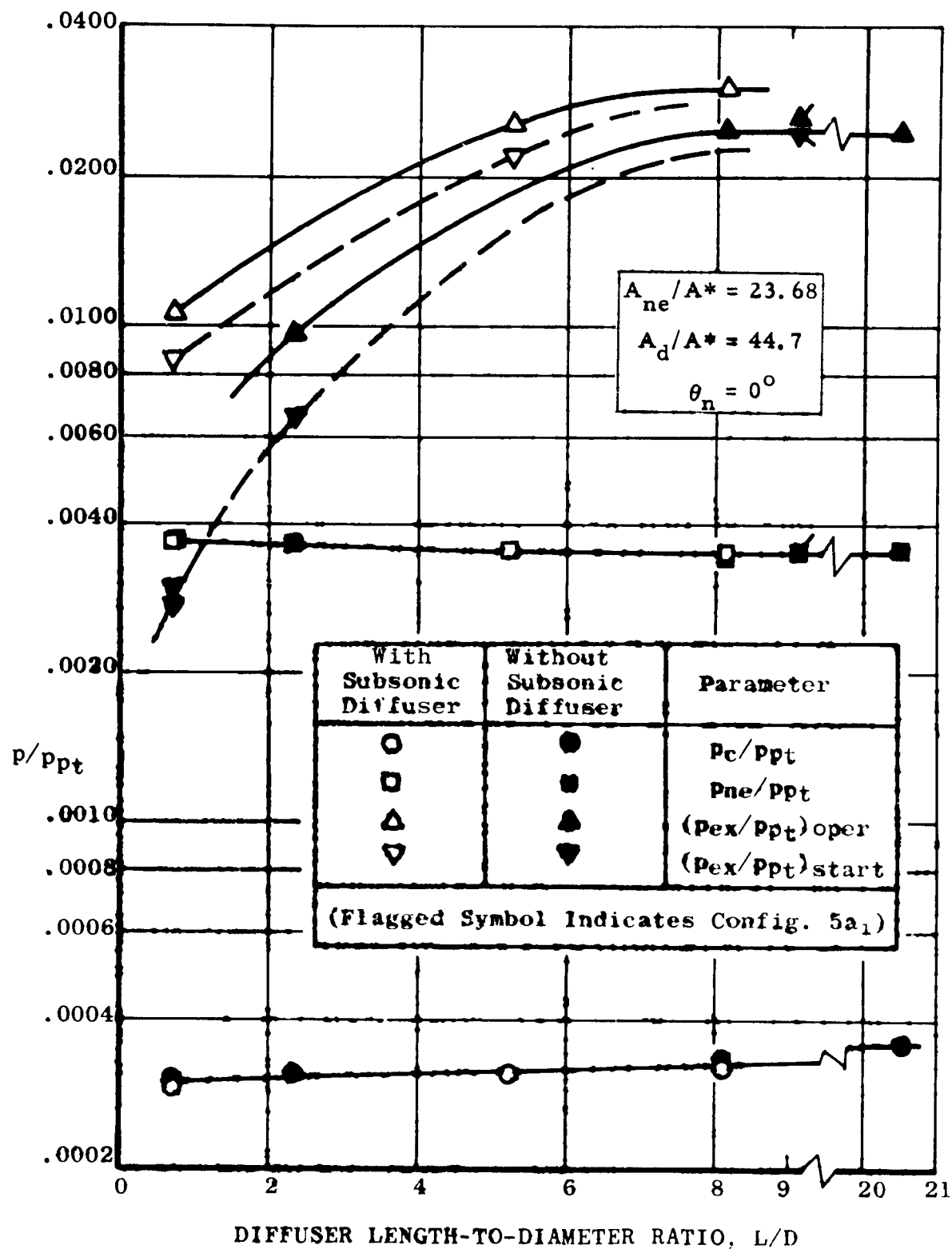
b. Configurations 3a, 3a₁, and 3a₁; $p_{p_1} = 45$ psia

Fig. 7 Continued



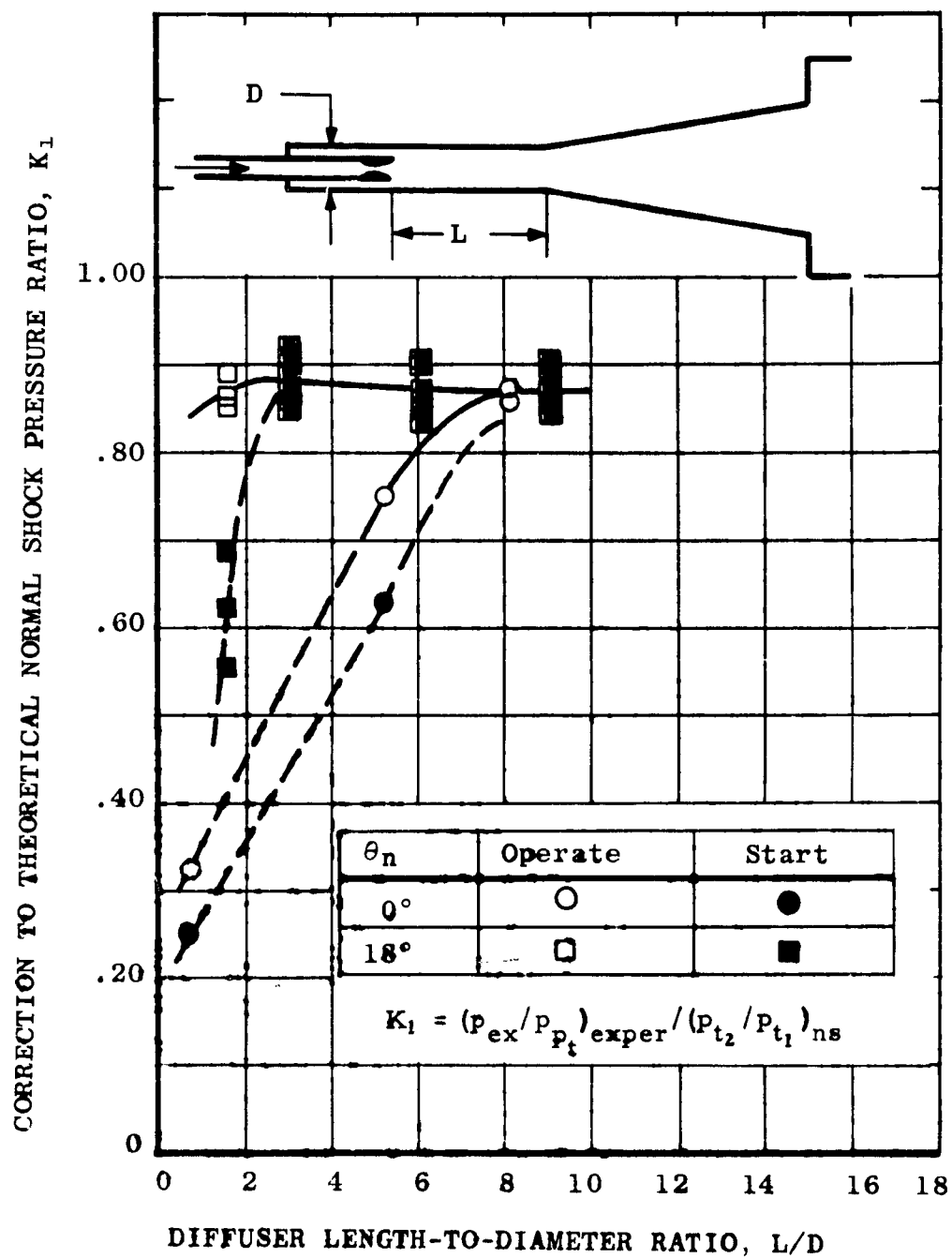
c. Configurations 4a and 4a1; $p_{p1} = 45$ psia

Fig. 7 Continued



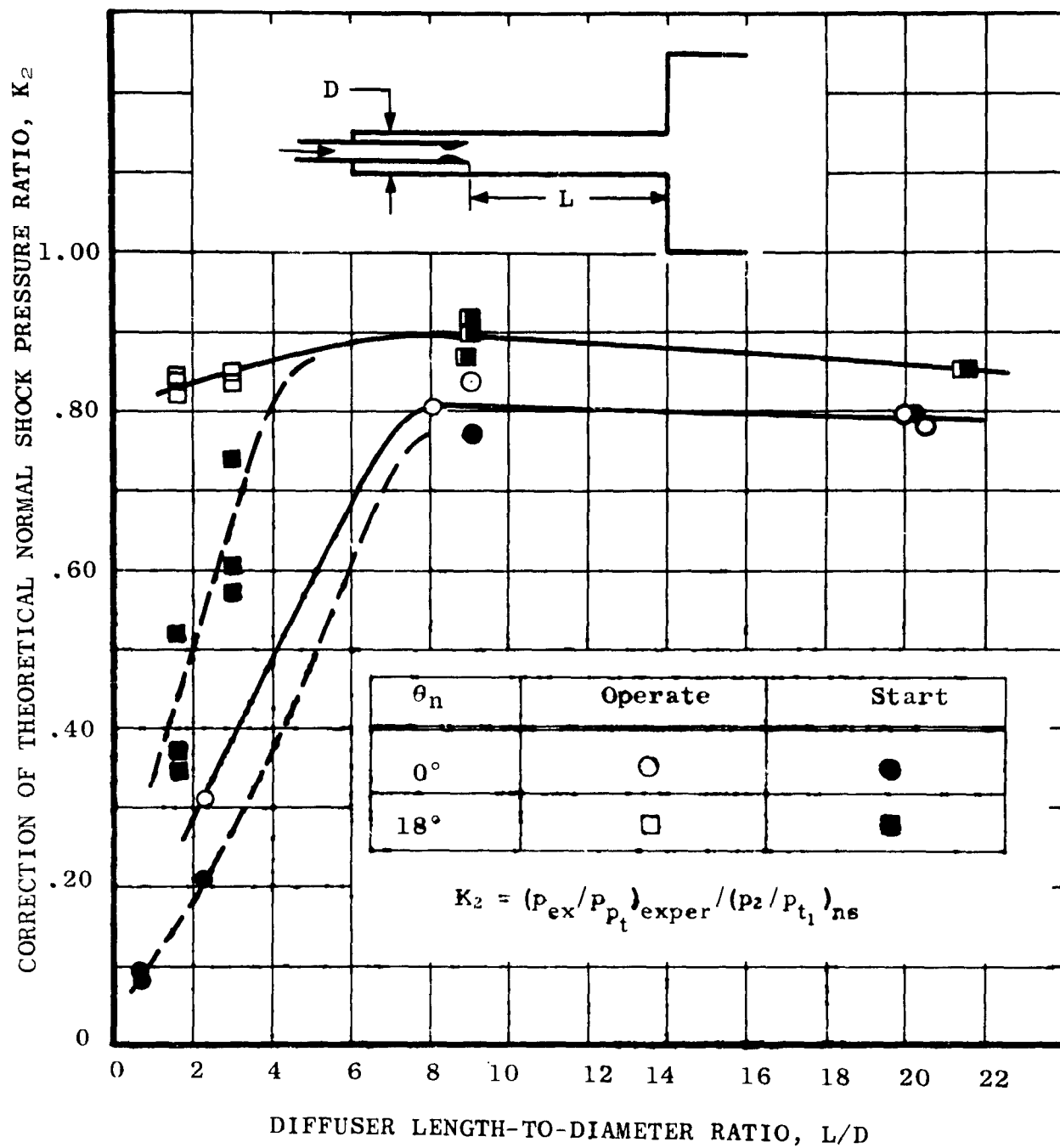
d. Configurations 5a, 5a₁, and 5a₁; $p_{p1} = 45$ psia

Fig. 7 Concluded



a. With Subsonic Diffuser

Fig. 8 Variation of Starting and Operating Pressure Ratio Correction Factor with Diffuser Length-to-Diameter Ratio, L/D , for $\theta_n = 0-18$ deg



b. Without Subsonic Diffuser

Fig. 8 Concluded

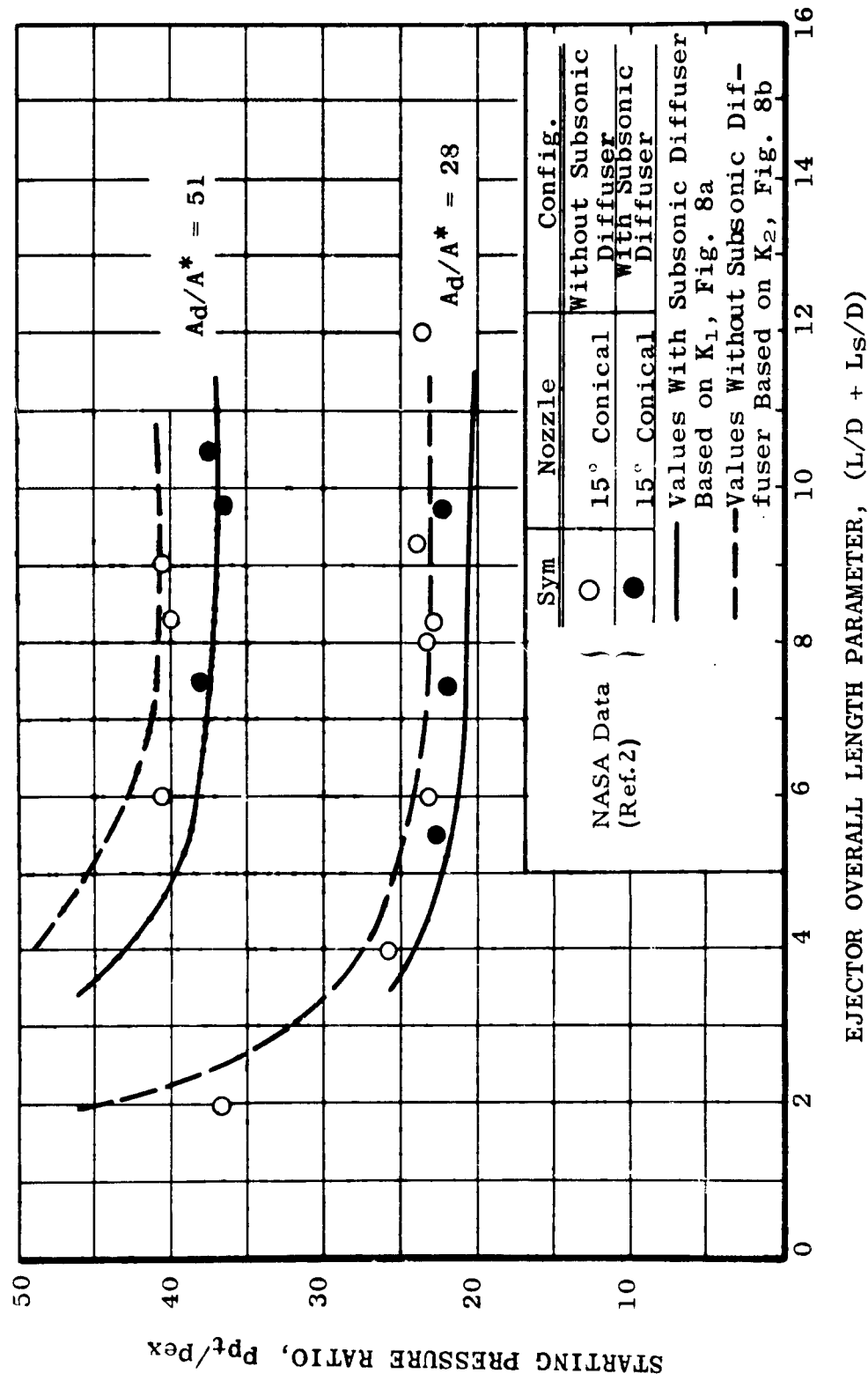
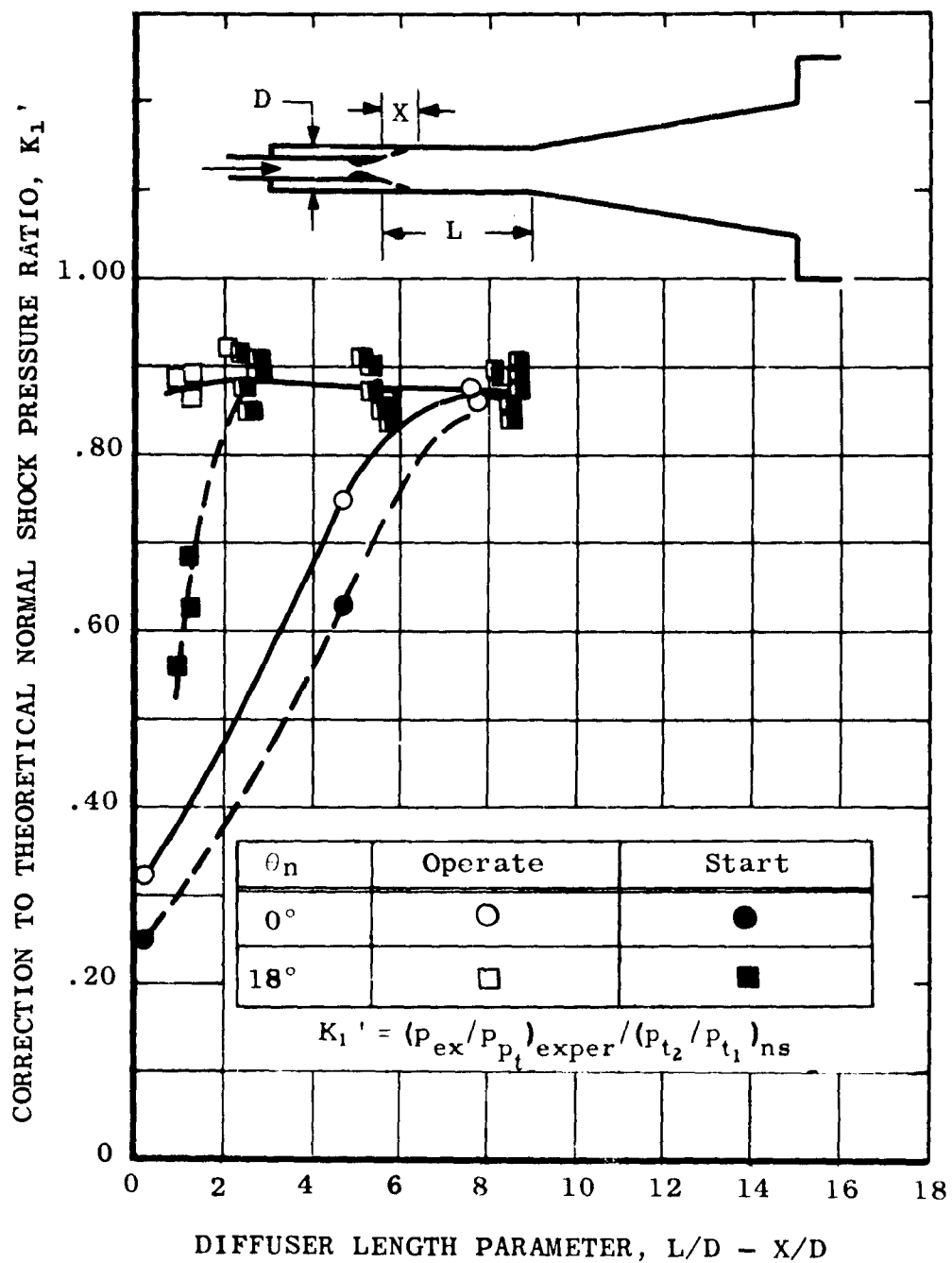
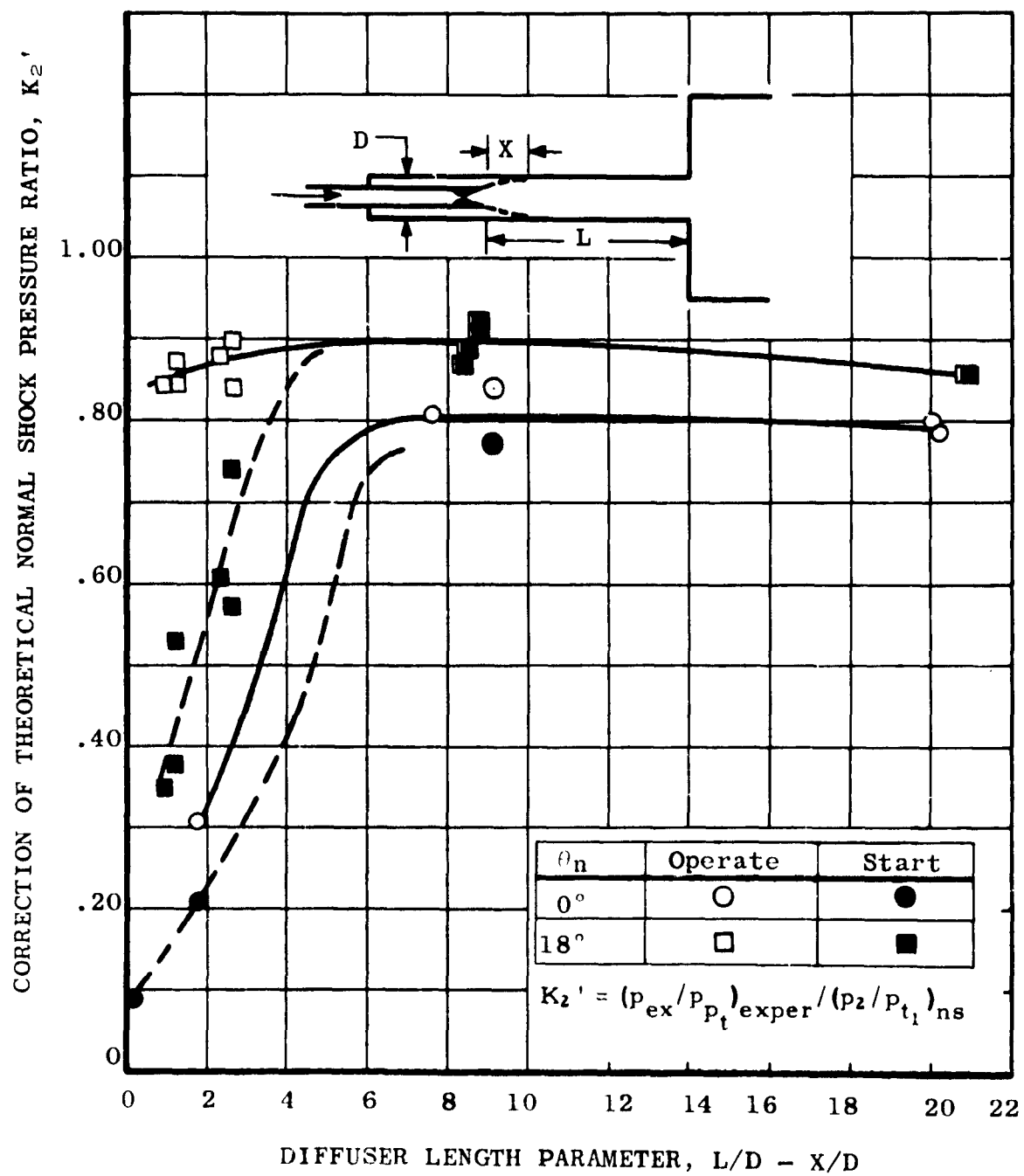


Fig. 9 Comparison of Estimated Starting Pressure Ratio and NASA Data (Ref. 2)



a. With Subsonic Diffuser

Fig. 10 Variation of Starting and Operating Pressure Ratio Correction Factor with Diffuser Length Parameter, $L/D - X/D$, for $\theta_n = 0-18$ deg



b. Without Subsonic Diffuser

Fig. 10 Concluded

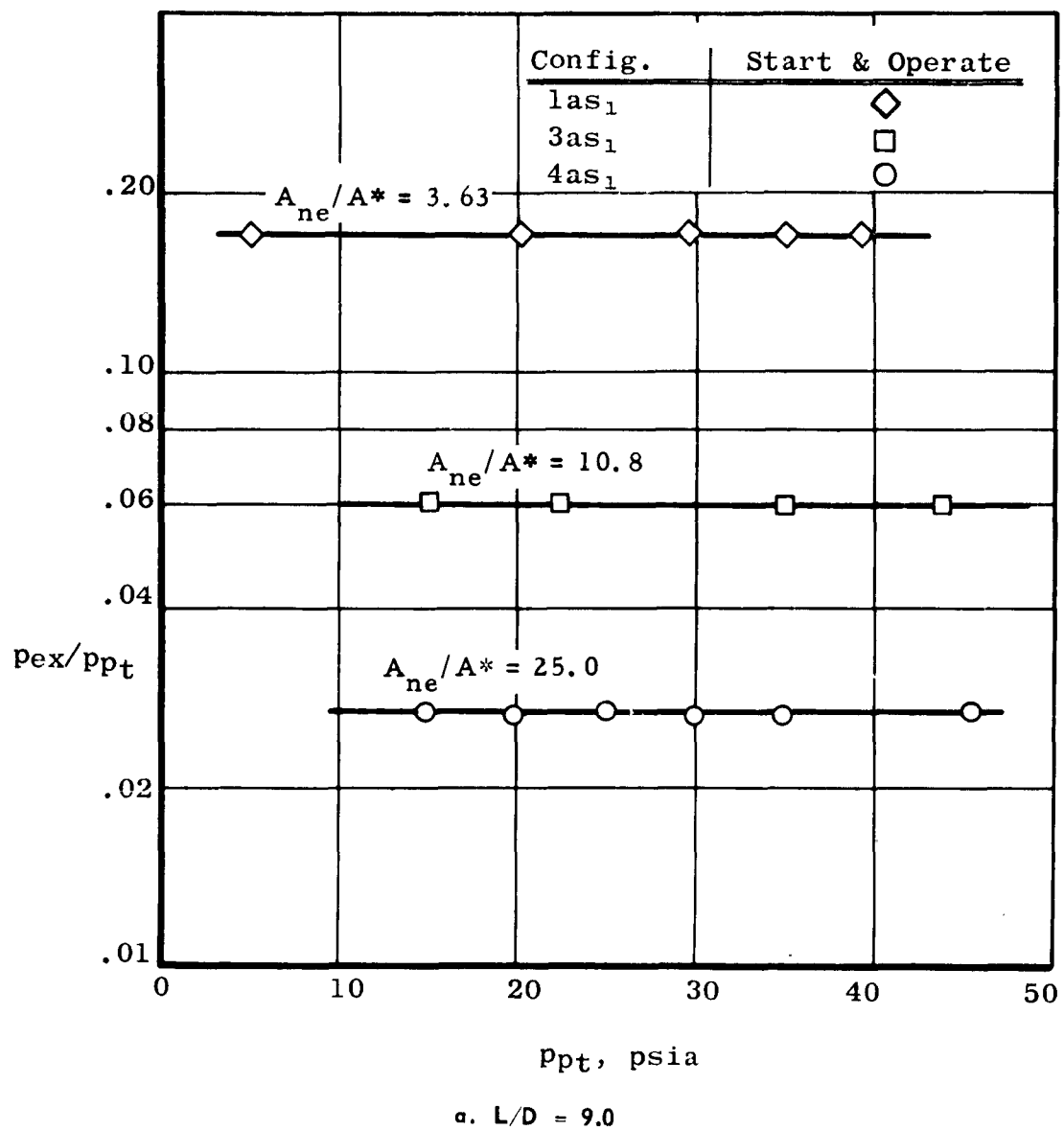
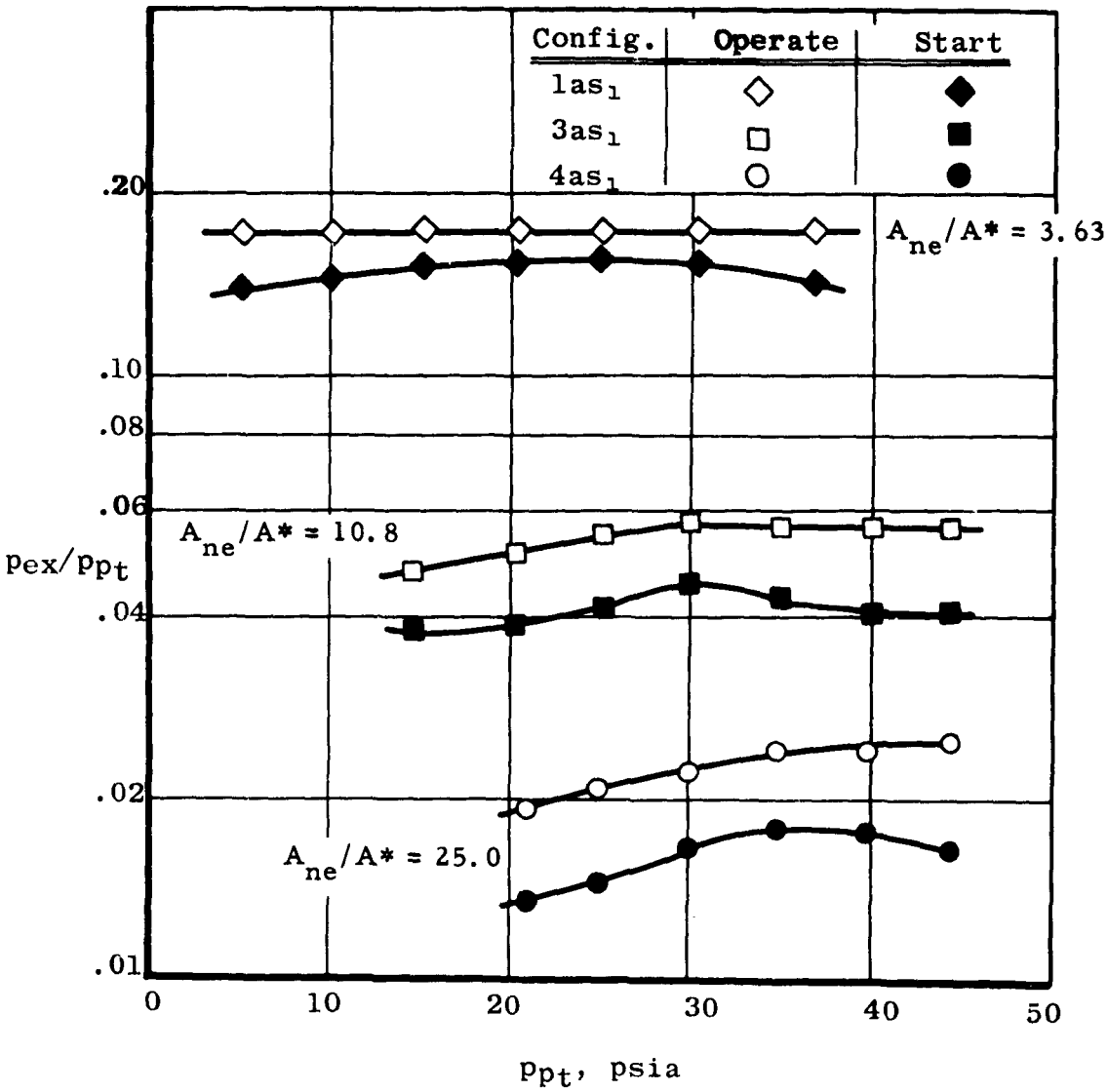


Fig. 11 Starting and Operating Pressure Ratio Variation with Total Pressure



b. $L/D = 1.6$
Fig. 11 Concluded

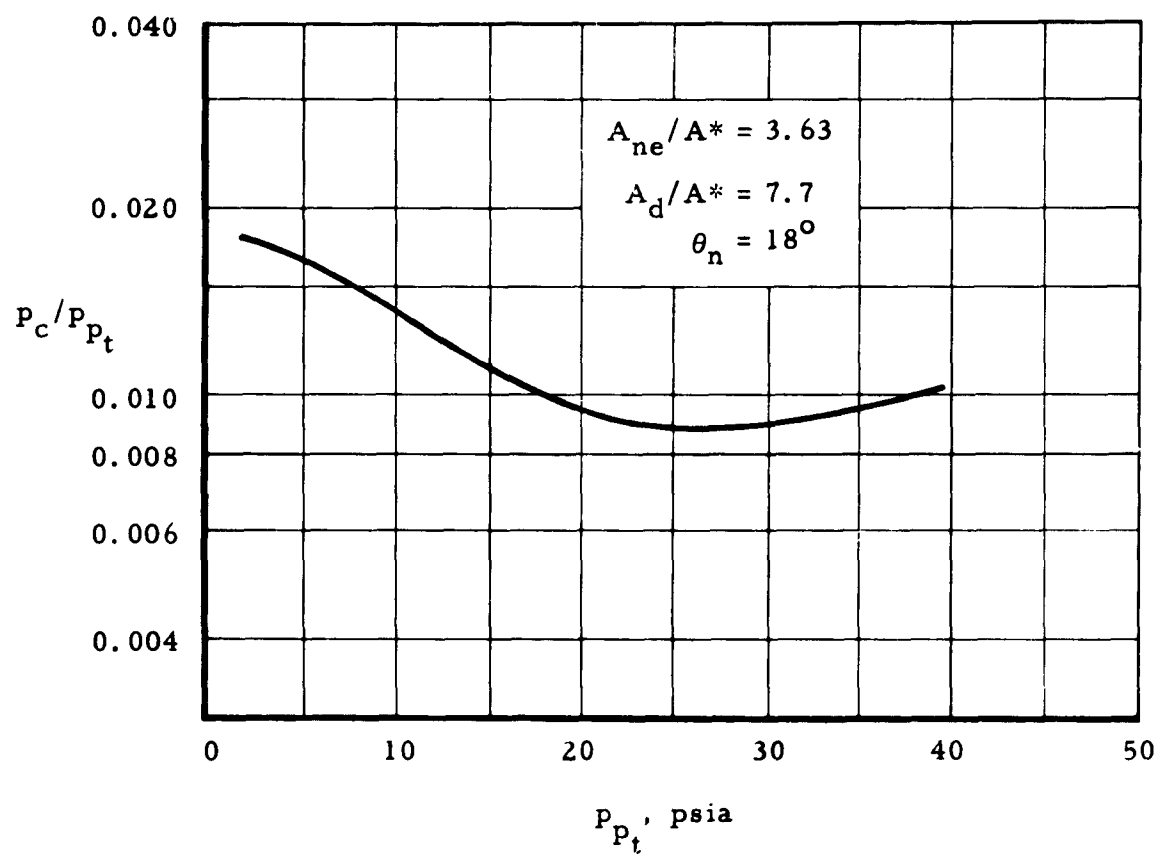


Fig. 12 Typical Cell Pressure Ratio Variation with Nozzle Plenum Total Pressure

Cut on broken line

<p>AEDC-TN-61-89</p> <p>Arnold Engineering Development Center, ARO, Inc., Arnold Air Force Station, Tennessee EFFECTS OF DIFFUSER LENGTH ON THE PERFORMANCE OF EJECTORS WITHOUT INDUCED FLOW by R. C. German and R. C. Bauer, August 1961. 43 pp. (ARO Project No. 100928) (AFSC Program Area 750G, Project 6950, Task 69501) (AEDC-TN-61-89) (Contract No. AF 40(600)-800 S/A 24(61-73)).</p> <p>Unclassified</p> <p>7 references</p> <p>An investigation of ejectors without induced flow was made to determine the effects of varying diffuser lengths on ejector performance. Four 18-deg half angle conical nozzles having constant exit diameters and different throat diameters and two contoured nozzles having zero-deg half angles at the exit were used as the ejector driving nozzles. Unheated air was used for all tests. The diffuser length-to-diameter ratios were varied between 0.7 and 21.5, and (over)</p>	<p>UNCLASSIFIED</p> <p>1. Ejectors--Performance 2. Diffusers-- Configurations I. German, R. C. II. Bauer, R. C.</p>
<p>AEDC-TN-61-89</p> <p>Arnold Engineering Development Center, ARO, Inc., Arnold Air Force Station, Tennessee EFFECTS OF DIFFUSER LENGTH ON THE PERFORMANCE OF EJECTORS WITHOUT INDUCED FLOW by R. C. German and R. C. Bauer, August 1961. 43 pp. (ARO Project No. 100928) (AFSC Program Area 750G, Project 6950, Task 69501) (AEDC-TN-61-89) (Contract No. AF 40(600)-800 S/A 24(61-73)).</p> <p>Unclassified</p> <p>7 references</p> <p>An investigation of ejectors without induced flow was made to determine the effects of varying diffuser lengths on ejector performance. Four 18-deg half angle conical nozzles having constant exit diameters and different throat diameters and two contoured nozzles having zero-deg half angles at the exit were used as the ejector driving nozzles. Unheated air was used for all tests. The diffuser length-to-diameter ratios were varied between 0.7 and 21.5, and (over)</p>	<p>UNCLASSIFIED</p> <p>1. Ejectors--Performance 2. Diffusers-- Configurations I. German, R. C. II. Bauer, R. C.</p>
<p>AEDC-TN-61-89</p> <p>Arnold Engineering Development Center, ARO, Inc., Arnold Air Force Station, Tennessee EFFECTS OF DIFFUSER LENGTH ON THE PERFORMANCE OF EJECTORS WITHOUT INDUCED FLOW by R. C. German and R. C. Bauer, August 1961. 43 pp. (ARO Project No. 100928) (AFSC Program Area 750G, Project 6950, Task 69501) (AEDC-TN-61-89) (Contract No. AF 40(600)-800 S/A 24(61-73)).</p> <p>Unclassified</p> <p>7 references</p> <p>An investigation of ejectors without induced flow was made to determine the effects of varying diffuser lengths on ejector performance. Four 18-deg half angle conical nozzles having constant exit diameters and different throat diameters and two contoured nozzles having zero-deg half angles at the exit were used as the ejector driving nozzles. Unheated air was used for all tests. The diffuser length-to-diameter ratios were varied between 0.7 and 21.5, and (over)</p>	<p>UNCLASSIFIED</p> <p>1. Ejectors--Performance 2. Diffusers-- Configurations I. German, R. C. II. Bauer, R. C.</p>

<p>AEDC-TN-61-89</p> <p>three cylindrical ducts of different diameters were used both with and without a subsonic diffuser. An empirical method was developed to estimate the starting and operating pressure ratios of such ejector configurations using simply-determined one-dimensional normal shock relationships.</p>	<p>UNCLASSIFIED</p>
<p>AEDC-TN-61-89</p> <p>three cylindrical ducts of different diameters were used both with and without a subsonic diffuser. An empirical method was developed to estimate the starting and operating pressure ratios of such ejector configurations using simply-determined one-dimensional normal shock relationships.</p>	<p>UNCLASSIFIED</p>